Geologia Croatica	65/2	109–138	33 Figs.	1 Tab.		Zagreb 2012

Bio- and Sequence Stratigraphy of Upper Cretaceous – Palaeogene rocks, East Bahariya Concession, Western Desert, Egypt

Mohamed Mahsoub[1], Radwan A.bul-Nasr[1], Mohamed Boukhary[2], Hamed Abd El Aal[1] and Mahmoud Faris[3]

[1] Faculty of Education, Ain Shams University, Cairo, Egypt; (mahsoub2005@hotmail.com; rabulnasr@yahoo.com; mabdelaal81@yahoo.com)

[2] Department of Geology Faculty of Science, Ain Shams University, Cairo, Egypt; (moboukhary@yahoo.com)

[3] Department of Geology Faculty of Science, Tanta University, Tanta, Egypt; (mhmfaris@yahoo.com)

doi: 104154/gc.2012.09

Geologia Croatica

ABSTRACT

This work deals with the plankton stratigraphy of the subsurface Upper Cretaceous-Palaeogene succession of the East Bahariya Concession based on planktonic foraminifera and calcareous nannofossils. The examination of the cuttings from five wells: AQSA-1X, KARMA-E-1X, KARMA-3X, KARMA-NW-1X and KARMA-NW-5X is biostratigraphically evaluated. It is possible to identify the planktonic foraminifera as well as the calcareous nannofossil biozones. The analyses of calcareous nannofossils revealed the presence of several hiatuses. Information obtained from well data such as seismic facies analysis for the studied area has enabled classification of the Upper Cretaceous-Palaeogene succession into five major 2nd order depositional sequences, separated by four major depositional sequence boundaries (SB1, SB2, SB3 and SB4). The Upper Cretaceous-Palaeogene succession in the East Bahariya is divided into 17 systems tracts. These systems tracts are: 7 System tracts of probable Cenomanian age, (the sequence stratigraphic framework as well as the cycles and system tracts of the Cenomanian Bahariya Formation match well with those of CATUNEANU et al., 2006); 4 System tracts of Turonian age, 2 System tracts of Campanian-Maastrichtian age and 4 System tracts of Eocene age.

Keywords: Planktonic foraminifera, Calcareous nannofossil, Upper Cretaceous, Palaeogene, Seismic interpretation, Sequence stratigraphy, Bahariya, Egypt

1. INTRODUCTION

The Western Desert of Egypt covers an area of approximately 700, 000 km^2, which represents two thirds of the total area of the country (EGPC, 1992).

The study area (Fig. 1) covers the Karama Field in the East Bahariya concession (EBC), located in the eastern margin of the Abu Gharadig Basin. The Karama Field was discovered in January 2000 by Repsol and Apache, while drilling the Karama 1-X well, which produced oil from the Abu Roash Member.

The Abu Gharadig Basin is located in the central northern part of the Western Desert. Topographically the Abu Gharadig Basin can be subdivided into two main troughs, the western and eastern trough. This basin is recently considered to be the most promising of all as far as hydrocarbon potential is concerned since several oil and gas discoveries had been recorded within its thick marine Cretaceous sequence (AWAD, 1984).

The aim of the present work is the study of the planktonic foraminiferal and calcareous nannoplankton biostratig-

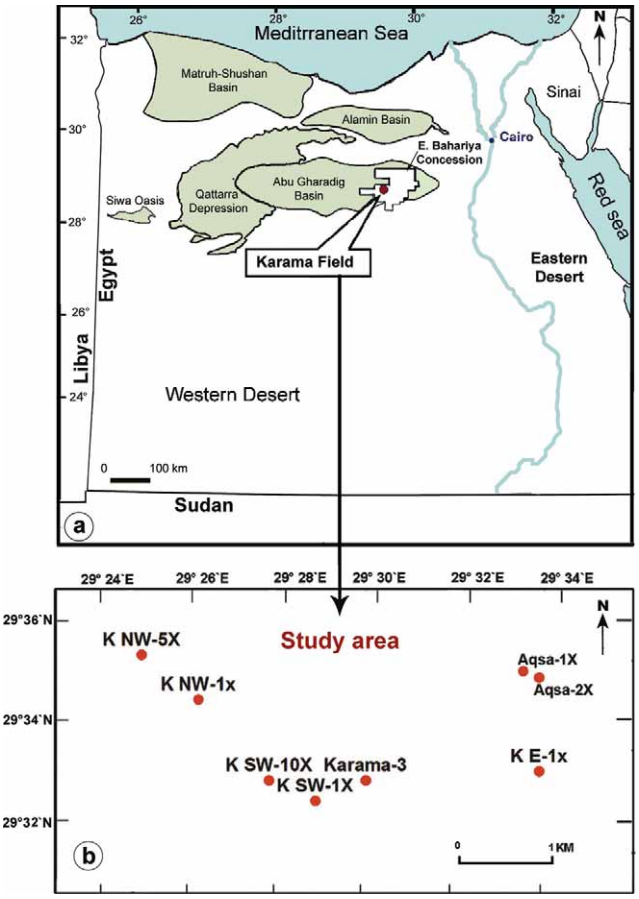

Figure 1: Location map of the area under study (a, b).

raphy of the Upper Cretaceous – Palaeogene rock units in the eastern part of the Bahariya concession and to integrate this data with that obtained from the seismic sections.

2. MATERIALS AND METHODS

Altogether 40 seismic sections were interpreted in order to illustrate the structural framework and depositional history of the study area. These seismic lines were supported by the composite, velocity and vertical seismic profile (VSP) logs of eight selected wells (AQSA-1X, AQSA-2X, KARAMA-E-1X, KARAMA-3X, KARAMA-SW-1X, KARAMA-SW-10X, KARAMA-NW-1X and KARAMA-NW-X).

Cuttings from five wells were selected for biostratigraphic studies that include several species of planktonic foraminifera and calcareous nannofossils.

Table 1: Shows the number and depth of the cuttings from the studied wells.

Wells	Depth interval (m)	No. of samples
AQSA-1X	338.4–2640	40
KARAMA-E-1X	365–2830	40
KARAMA-3X	365–2470	40
KARAMA-NW-1X	430–2600	40
KARAMA-NW-5X	450–2600	40

3. STRATIGRAPHY

The surface of the northern part of the Western Desert is covered by Miocene deposits, except for the Bahariya and Abu Roash areas that are covered with Upper Cretaceous and Eocene sediments (Fig. 2). In the Fayium area both Eocene and Oligocene limestones, clays and sandstones dominate the section. In the Bahariya and Fayium areas Oligocene volcanic basalt makes up a substantial part of the geological succession. The Miocene deposits are subdivided into the lower Miocene Moghra Formation and the Middle Miocene Marmarica Formation (SAID, 1962).

Based on the surface geological map of the Western Desert, the Miocene deposits are separated from the Eocene rocks in the south by a narrow band of Oligocene carbonates at Siwa (HARPE DE LA, 1883) while in Al Arag there is a gradual southerly change into a clastic succession at Bahariya and Fayium (OSMAN, 2003).

The Miocene surface usually doesn't usually reflect structures at depth as an angular unconformity is observed at many places separating the Miocene and underlying Eocene deposits. The Upper Eocene deposits occupied mainly the

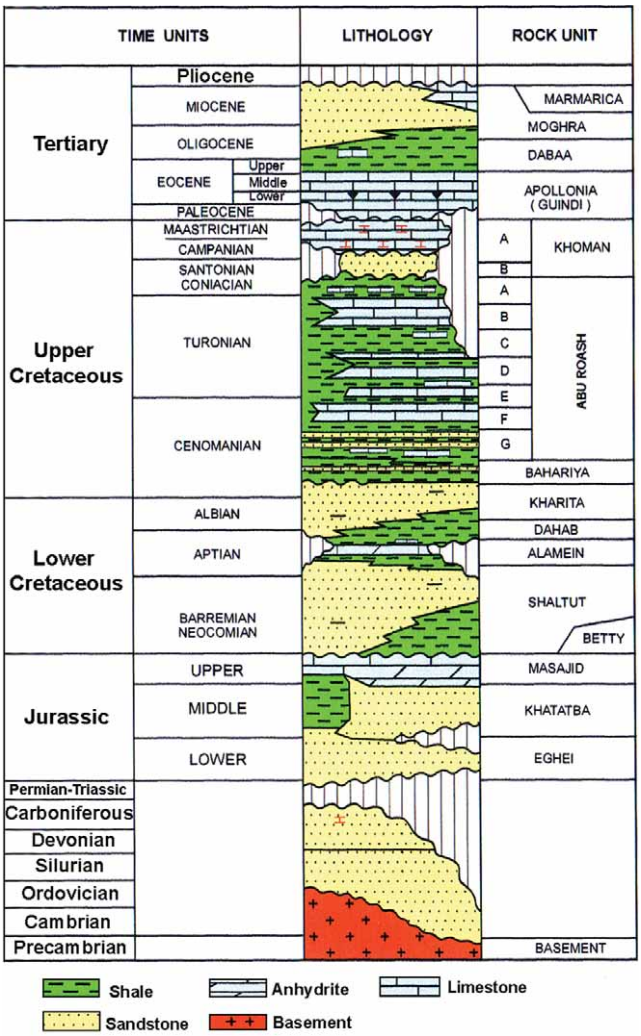

Figure 2: Generalized lithostratigraphic column in the Abu Gharadig Basin.

central and the south eastern parts of the Western Desert. These marine deposits are mainly limestone represented by the Thebes and farafra Formations, the former representing an open marine facies while the latter is a shallow shelf lithofacties (SAID, 1960). The Cretaceous deposits are mainly located at the southern part of the Western Desert and they consist mainly of the Nubia Formation.

3.1. Subsurface stratigraphy of the Western Desert

The subsurface lithostratigraphic column in the northern part of the Western Desert contains most of the sedimentary section from Pre-Cambrian basement rocks to Recent deposits. The total thickness of the sedimentary section measures about 4270 m (YOUNES, 2003). Figure 2 summarizes the main stratigraphic units in the Abu Gharadig basin of the Western Desert.

3.1.1. Upper Cretaceous rocks

In Egypt, the Upper Cretaceous is marked by the beginning of a major marine transgression which resulted in the deposition of a carbonate dominated section in the study area. According to ISSAWI et al. (1999), the Upper Cretaceous succession is subdivided into three lithostratigraphic units from the oldest Bahariya, to the Abu Roash and the Khoman Formations.

The sedimentary rocks of the Upper Cretaceous occur in three basins of the Western Desert; the Abu Gharadig, Shushan, and Alamin basins, which include the most important hydrocarbon resources in the Western Desert. The formations are discussed from oldest to youngest below.

3.1.1.1. Bahariya Formation

The type locality of this unit is located in the Gabel El Dist (Bahariya Oasis) where the base of the formation is not exposed at the surface. The maximum thickness of this formation occurs in the Kattaniya-1 well (1143 m) (29° 49'N and 30° 10'E). The name of this unit was proposed by SAID (1962), STROMER (1914a, b) and SMITH et al., 2006 based on dinosaurs remain for the lower Cenomanian fluvio-marine (CATUNEANU, 2006) sediments which consist of argillaceous sandstone with some carbonates.

3.1.1.2. Abu Roash Formation

The type locality of the Abu Roash Formation outcrops to the north of the Pyramids of Giza (30° 2' 44.59"N and 31°14' 24.71"E). This unit is subdivided into seven lithostratigraphic members, termed from top to bottom as A, B, C, D, E, F, and G, which extend from the Santonian to the Upper Cenomanian. Most of the facies were deposited under neritic to open marine, basinal conditions. The Abu Roash represents the alternation of transgressive and regressive phases, characterized by:

1. Shallow to deeper marine carbonates on palaeohighs. The limestones-were dolomitized and have fracture porosity.
2. Shallow deposits, consisting of the alternation of shales and sandstones. During Turonian times, an evaporitic sequence was deposited in some areas.

Lithologically, this unit consists of white moderately hard fossiliferous, cherty, massively bedded, micro-to cryptocrystalline chalky limestone. The shales are gray, dark brown and greenish in colour with moderate hardness, containing some glauconite and pyrite. Dolomite is brownish in colour, buff, massive and moderate in hardness. This reflects a nearshore or Sabkha type of depositional environment.

3.1.1.3. Khoman Formation

The type section of this unit is located at Ain Khoman, southwest of the Bahariya Oasis. It represents an open marine facies which prevailed in the north Western Desert during the Campanian and Maastrichtian and it unconformably overlies the Abu-Roash Fm., particularly in the structurally highest area. Lithologically this formation consists of two main units: the lower unit is mostly limestone interbedded with shale, the limestone is massive, white dolomitic limestone and the shale is brownish, gray with medium hardness while the upper, unit is of fine-grained white chalky massive limestone and massive dolomite and lacks of adequate reservoir properties.

3.1.2. Cenozoic rocks

At the end of Cretaceous, sedimentation in the Western Desert was continuous in the structurally low and subsiding areas while some depositional gaps and erosional truncations were common on the pre-existing highs, which were reactivated, especially during the Palaeocene (SCHLUMBERGER, 1984).

Palaeogene rocks include the Palaeocene to Middle Eocene Apollonia Fm. which consists mainly of shallow to open marine carbonates. The Upper Eocene to Oligocene Dabaa Fm. consists of shallow marine shales and the Miocene Moghra Fm. consists mainly of shallow to marginal marine sandstones with thin shale interbeds and a basalt extrusion near its top. The basal part of the Moghra Fm. laterally changes to carbonates (Shoushan Formation) in the northwest portion of the Western Desert. The Oligo-Miocene rocks are also overlain by the middle Miocene Marmarica Fm. to the northwest of the Western Desert, which consists of shallow marine carbonates (NORTON, 1967; ABDEL AAL & MOUSTAFA, 1988). Quaternary deposits unconformably overlie the Miocene rocks and consist of Plio-Pleistocene continental sands.

3.1.2.1. The Apollonia Formation

This is a widespread limestone with subordinate shale of Palaeocene to Eocene age. The type locality is located south of the village of Susa (32° 53' 48"N and 21° 57' 47"E) in Libya. The type section is 250 m thick and is made up of massive siliceous limestones with numerous chert bands.

The lithology is white, chalky limestone, in many places nummulitic, with some shaly zones, especially where the formation is thick. Glauconite and pyrite are common and widespread. Chert nodules occur, and are common in the lower part. The formation has been subdivided by several operators into units A to D where D is the oldest. Units B and D are thinner and dominanted by shale.

3.1.2.2. The Dabaa Formation

The type section is the interval 579 to 1021 m interval of the Dabaa-1 well. Lithologically it is composed of gray and greenish-gray clay and claystone with subordinate thin beds of limestone, glauconite and pyrite minerals, of Upper Eocene to Oligocene age.

The majority of the wells drilled in the study area revealed the same stratigraphic column of the North-Western Desert with a few exceptions in the variations of thickness and the absence of some rock units.

4. BIOSTRATIGRAPHY

Cuttings from five wells (AQSA-1X, KARAMA-E-1X, KARAMA-3X, KARAMA-NW-1X and KARAMA-NW-5X) were selected for study and the identification of microfossils. Several species of planktonic foraminifera and calcareous nannofossils have been identified. Some stratigraphically important taxa are illustrated (Figs. 8–11 and Figs. 17–21).

Calcareous nannofossils were processed by the standard smear slide preparation from raw sediment samples as described by Perch-Nielsen (1985). Smear slides were examined using a light photomicroscope with 1250x objective. A relative abundance of calcareous nannofossils was used as follows: A= abundant more than 5 specimens /field of view (fov), C= common 1–5 specimens/fov, F= frequent one specimen /2–5 fov, R= rare one specimen/6–10 fov and VR= very rare one specimen/more 10 fov.

4.1. Planktonic and benthic foraminifera

The planktonic foraminifera were used to date the different successions of the studied wells. Most successions range in age from the Cretaceous (Cenomanian) to the Oligocene. Planktonic and benthic foraminifera are encountered only in the marine upper half of the succession which is represented, in ascending order, by the Khoman Fm, the Apollonia Fm, and the Dabaa Fm.

4.1.1. Preparation technique

Samples were soaked in Hexametaphosphate solution and then washed through a 0.64 mm sieve. The operation was repeated until the residue became clean. Hard samples were then treated by ultrasonic cleaner. Foraminiferal specimens were picked and mounted on squared slides for identification.

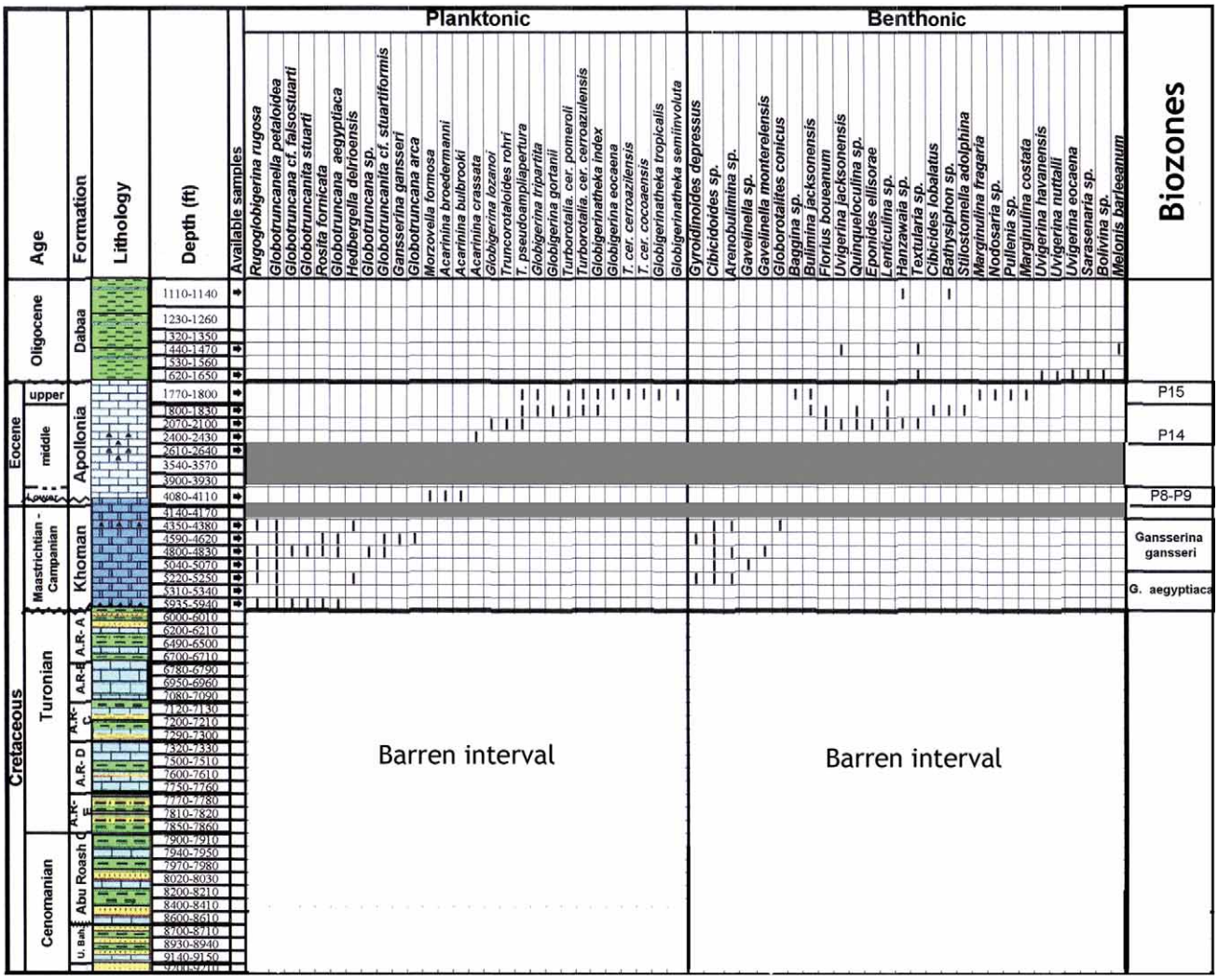

Figure 3: Distribution chart of the planktonic and benthic foraminifera of the Well Aqsa-1x.

Unconformity

4.1.2. The Khoman formation

The Khoman Formation contains planktonic and benthic foraminiferal assemblages of Campanian – Maastrichtian age (Figs. 3 to 7).

The faunal assemblages of the Khoman Fm. belong to the following planktonic foraminiferal zones, from base to top, as follows: *Globotruncana ventricosa* Zone, *G. aegyptiaca* Zone (CARON, 1985; CARON et al., 2006 and BERGGREN & PEARSON, 2006) and *Gansserina gansseri* Zone which are assigned to the Upper Campanian to Maastrichtian.

4.1.3. Apollonia Formation

The Apollonia Formation unconformably overlies the Khoman Formation. It consists mainly of limestone with occasional argillaceous interbeds in some wells. It is relatively poor in foraminifera and almost barren at some levels. Accordingly, systematic biozonation is difficult and impractical to establish, especially due to the absence of some key species (Figs. 3 and 7). However, some other species have helped in establishing different age divisions of the Apollonia Formation Figures 3 to 7 shows the distribution of planktonic foraminifera in the Apollonia Formation of the different wells. The Lower/Middle Eocene boundary has been drawn at the first appearance of Middle Eocene species such as *Acarinina bullbrooki* especially when associated with *Catapsydrax* sp and *Turborotalia cerroazulensis pomeroli*. The Lower Eocene is estimated according to the occurrence of only lower Eocene species such as *Morozovella formosa*, *Acarinina soldanii*, & *Acarinina pentacamerata*. These three species together with *Acarinina broedermanni* represent the assemblage of the Lower Eocene (BOLLI, 1957; TOUMARKINE & LUTERBACHER, 1985; BERGGREN & PEARSON, 2006). They are usually followed by a barren interval before the inception of the Middle Eocene species. Accordingly, the Lower/Middle Eocene boundary here is speculative rather than factual.

The Middle Eocene part is the interval richest interval in foraminifera. All the species of the assemblage support this age determination based on comparison with those mentioned in the literature (BOLLI, 1957 & BLOW, 1979; TOUMARKINE & LUTERBACHER, 1985; BERGGREN & PEARSON, 2006). It is worth mentioning, however, that except for *Acarinina* and *Truncorotaloides*, the range of these species extends to the Upper Eocene. Yet, the index species of the Upper Eocene, *Globigerinatheka semiinvoluta*, is used to delineate the Upper Eocene upon its occurrence. This species appears in some wells (Figs. 3 and 5) and is absent in others (Figs. 4, 6 and 7).

The latest Eocene fauna such as *Cribrohantkenina*, *T.c. cocoaensis*, *T.c. cunialensis* are absent from the material sug-

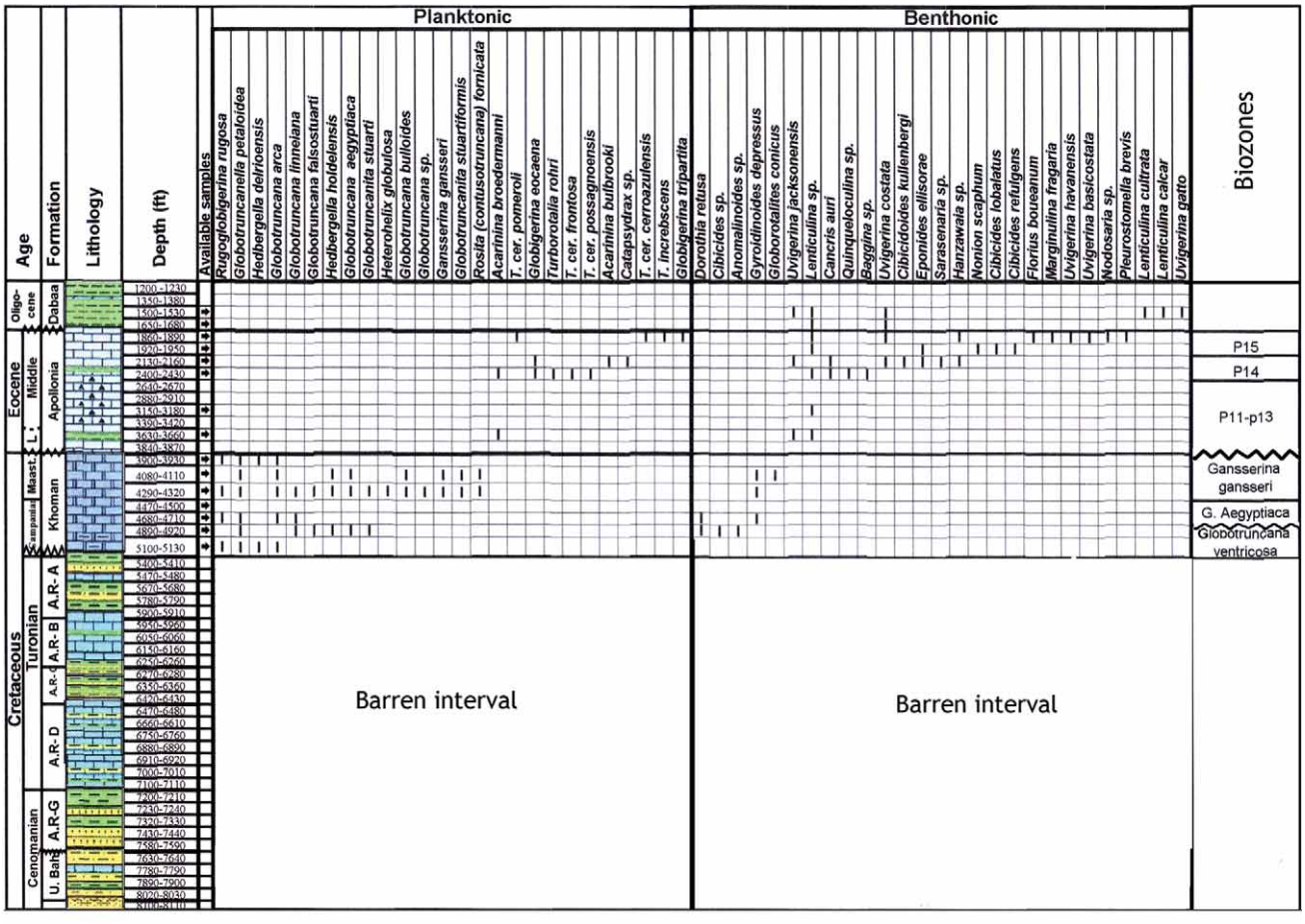

Figure 4: Distribution chart of the planktonic and benthic foraminifera of the Well Karama-3.

gesting that the Upper Eocene when observed is incomplete. Accordingly, the boundary between the Apollonia Fm. and the underlying Khoman Fm. is represented by a hiatus spanning the whole Palaeocene and the basal part of the Eocene with some hiatuses within the formation. The recorded planktonic foraminiferal zones: from the *Morozovella aragonensis* zone (P8, BOLLI, 1957 and TOUMARKINE & LUTERBACHER, 1985) to the *Globigerinatheka semiinvoluta* Zone (P15, Bolli, 1957) are delineated within the Apollonia Fm. With the pronounced unconformity with the overlying Dabaa Fm.

4.1.4. The Dabaa Formation

The Dabaa Fm. is devoid of identifiable planktonic foraminifera in spite of the sporadic occurrence of benthics species. So, its Oligocene age, as estimated by sporadic fauna, is adopted here. The planktonic and benthic species are shown in Figures 8 to 11.

4.2. Nannoplankton biostratigraphy

The zonations of SISSINGH (1977) for the Upper Cretaceous and that of MARTINI (1971) and OKADA & BUKRY (1980) for the Lower Palaeogene were adopted here in the deep wells, contamination by caving is observed through examination of the cutting. In the study wells, nannofossils are frequent to rare and moderately to poorly preserve.

In the following, the recognized nannofossil biozones are discussed from, base to top. Abbreviations used are: FO = First occurrence, LO = Last occurrence. FO is used following the standard biostratigraphic scheme but taking into consideration that the samples are cuttings; the law of first appearance is applied accordingly.

4.2.1. Upper Cretaceous calcareous nannofossil biostratigraphy

4.2.1.1. *Quadrum trifidium* Zone (CC22)

Definition: It is defined as the interval from the FO of *Quadrum trifidium* to the LO of *Reinhardtites anthophorous.*

Authors: BUKRY & BRAMLETTE (1970), emended by SISSINGH (1977)

Age: Late Campanian.

Occurrence: Aqsa-1x (1590–1800 m), Karama-3x (1500–1550 m), Karama-NW-1x(1450–1650 m) (in Khoman Formation).

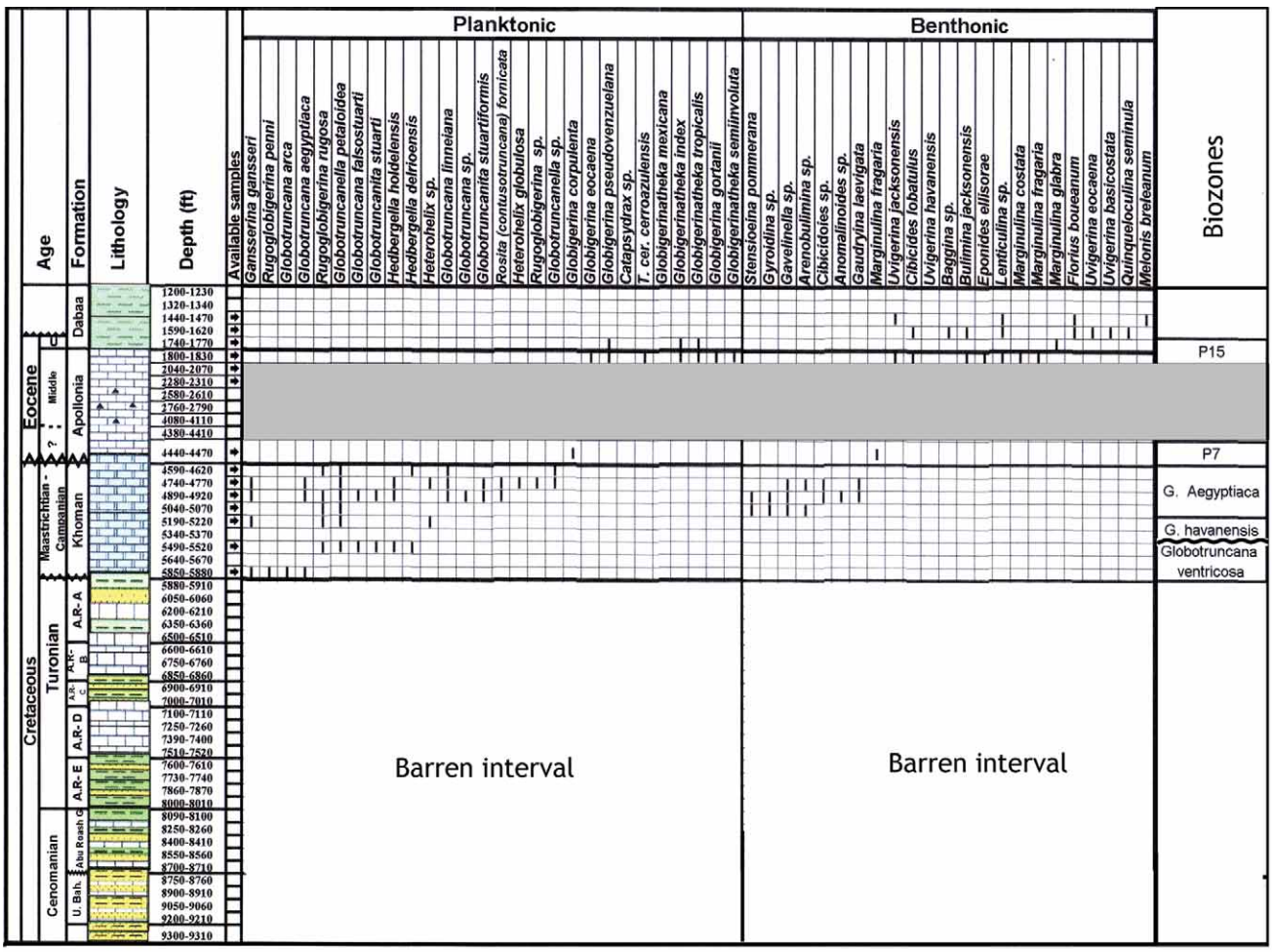

Figure 5: Distribution chart of the planktonic and benthic foraminifera of the Well Karama-E-1x.

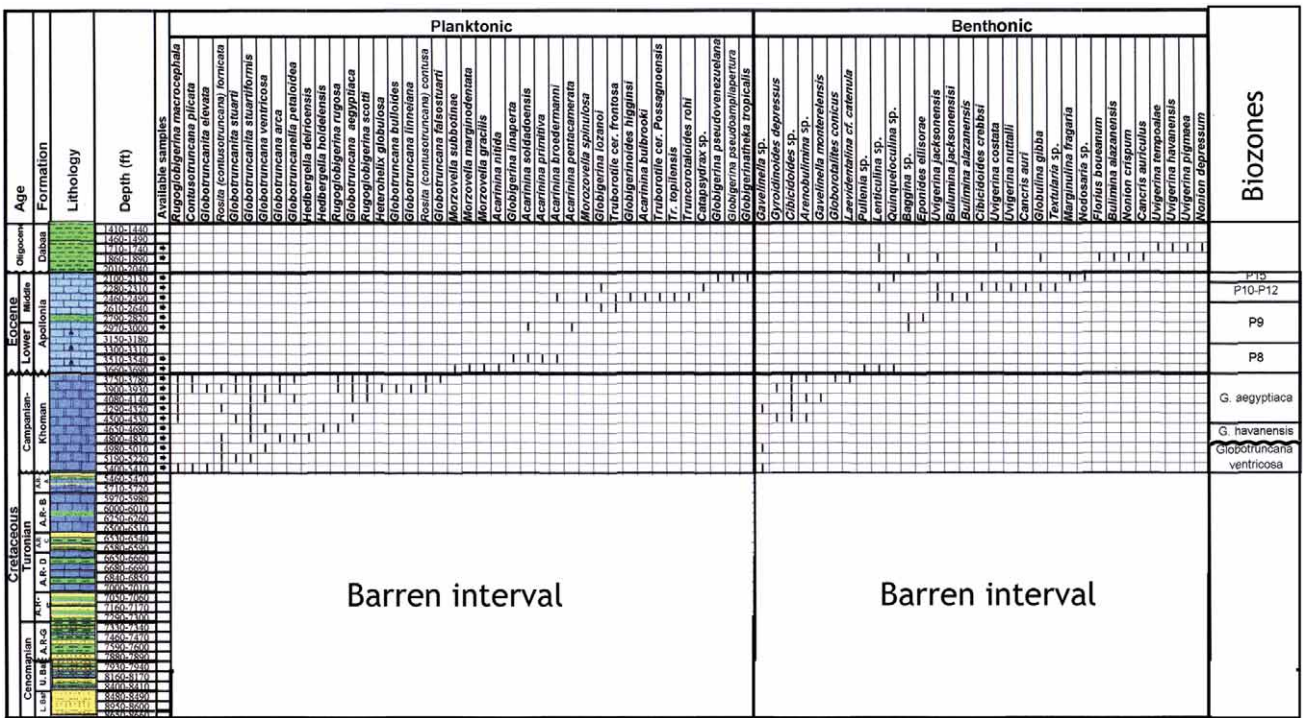

Figure 6: Distribution chart of the planktonic and benthic foraminifera of the Well Karama-NW-1x.

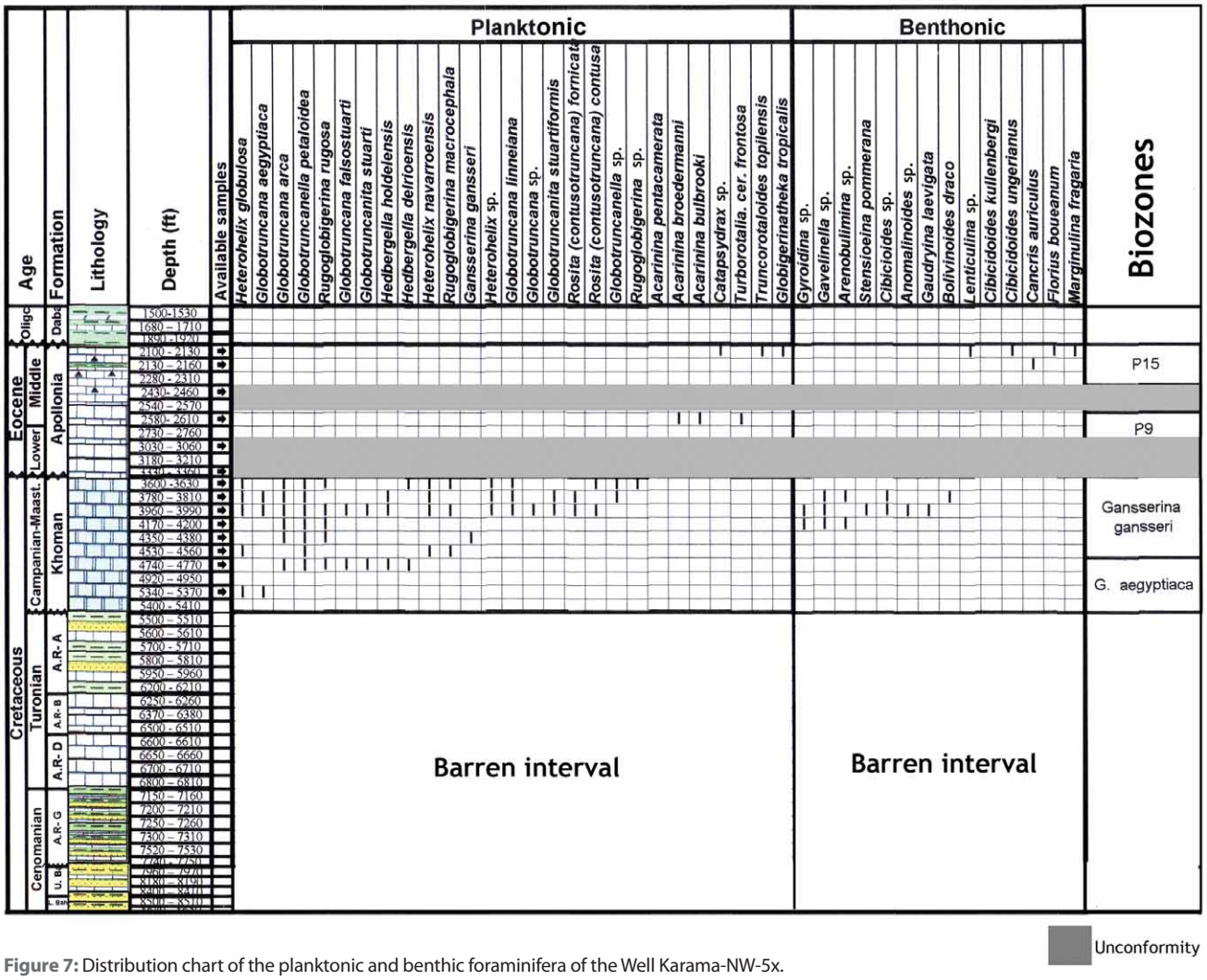

Figure 7: Distribution chart of the planktonic and benthic foraminifera of the Well Karama-NW-5x.

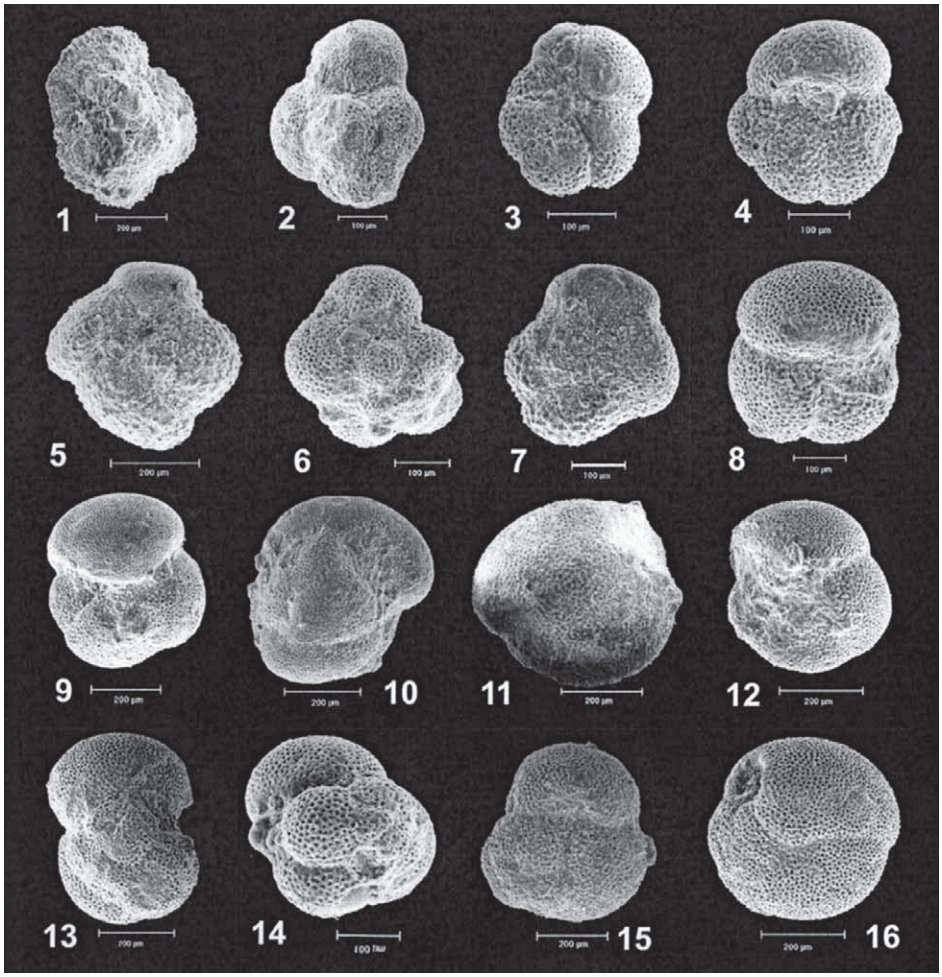

Figure 8: Planktonic Eocene plate. **1** – *Morzovella subbotinae* MOROZOVA, 1929; 3690 ft, Karama-NW-1x. **2** – *Globigerina eocaena* GUEMBEL1966; 1650 ft, Aqsa-1x. **3** – *Acarinina crassata* CUSHMAN, 1962; 2430 ft, Aqsa-1x. **4** – *Globigerina pseudoampliapertura* (BOW, BANNER, 1962); 2130 ft, Karama- NW-1x. **5–7** – *Acarinina crassata*, Toumarkine, BOLLI, (1970); 1800 ft, Aqsa-1x. **8** – *Turborotalia cerroazulensis possagnoensis*, Toumarkine, BOLLI, (1970); 2430 ft, Karama-3x. **9–11** – *Turborotalia cerroazulensis pomeroli*, Toumarkine, BOLLI, (1970); 1890 ft, Karama-3x. **12** – *Turborotalia cerroazulensis* BOLLI, (1970); 1830 ft, Karama-E-1x. **13** – Globigerinatheka index (finaly, 1939); 1770 ft, Karama- E-1x. **14,15** – *Globigerinatheka tropicalis* (BLOW, BANNER, 1962); 2130 ft, Karama- NW-1x. **16** – *Globigerinatheka semiinvoluta* (KEIJZER, 1945); 1830 ft, Karama- E-1x.

Remarks: In addition to the zonal marker, the nannofossil assemblage includes: *Watznaueria barnesae, Cyclagelosphaera reinhardtii, Lucianorhabdus*. *cayeuxii, Cribrosphaerella ehrenbergii, Aspidolithus parcus, Eiffellithus eximius*.

4.2.1.2. *Tranolithus phacelosus* Zone (CC23)

Definition: It is defined from the LO of *Reinhardtites anthophorus* to the LO of *Tranolithus phacelosus.*

Authors: SISSINGH (1977)

Age: Late Campanian to Early Maastrichtian.

Occurrence: Karama-3x (1370–1435 m), Karama-NW-1x (1150–1420 m) (in Khoman Formation).

Remarks: In addition to the zonal markers, the nannofossil assemblage includes the large sized forms of *Eiffellithus turiseffelii* and *Arkhangleskiella cymbiformis*.

4.2.1.3. *Arkhangleskiella cymbiformis* Zone (CC25)

Definition: It is defined from the LO of *Reinhardtites levis* to the FO of *Nephrolithus frequens*.

Authors: PERCH – NIELSEN (1972), emended by SISSINGH (1977)

Age: Late Maastrichtian.

Occurrence: Aqsa-1x (1400–1540 m), Karama-NW-5x (1700–1400 m) (in Khoman Formation).

Remarks: The CC25 Zone is unconformably overlain by zone NP12 (Early Eocene), with a marked hiatus spanning the uppermost Maastrichtian, as well as the entire Palaeocene and the lower part of the lower Eocene.

4.2.2. Lower Palaeogene calcareous nannoplankton biostratigraphy

4.2.2.1. *Tribrachiatus orthostylus* Zone (NP12)

Definition: The Base is defined by the first occurrence (FO) of *Discoaster lodoensis* and the top by the last occurrence of *Tribrachiatus orthostylus*.

Authors: BRÖNNIMANN & STRADNER (1960)

Age: Early Eocene (Ypresian).

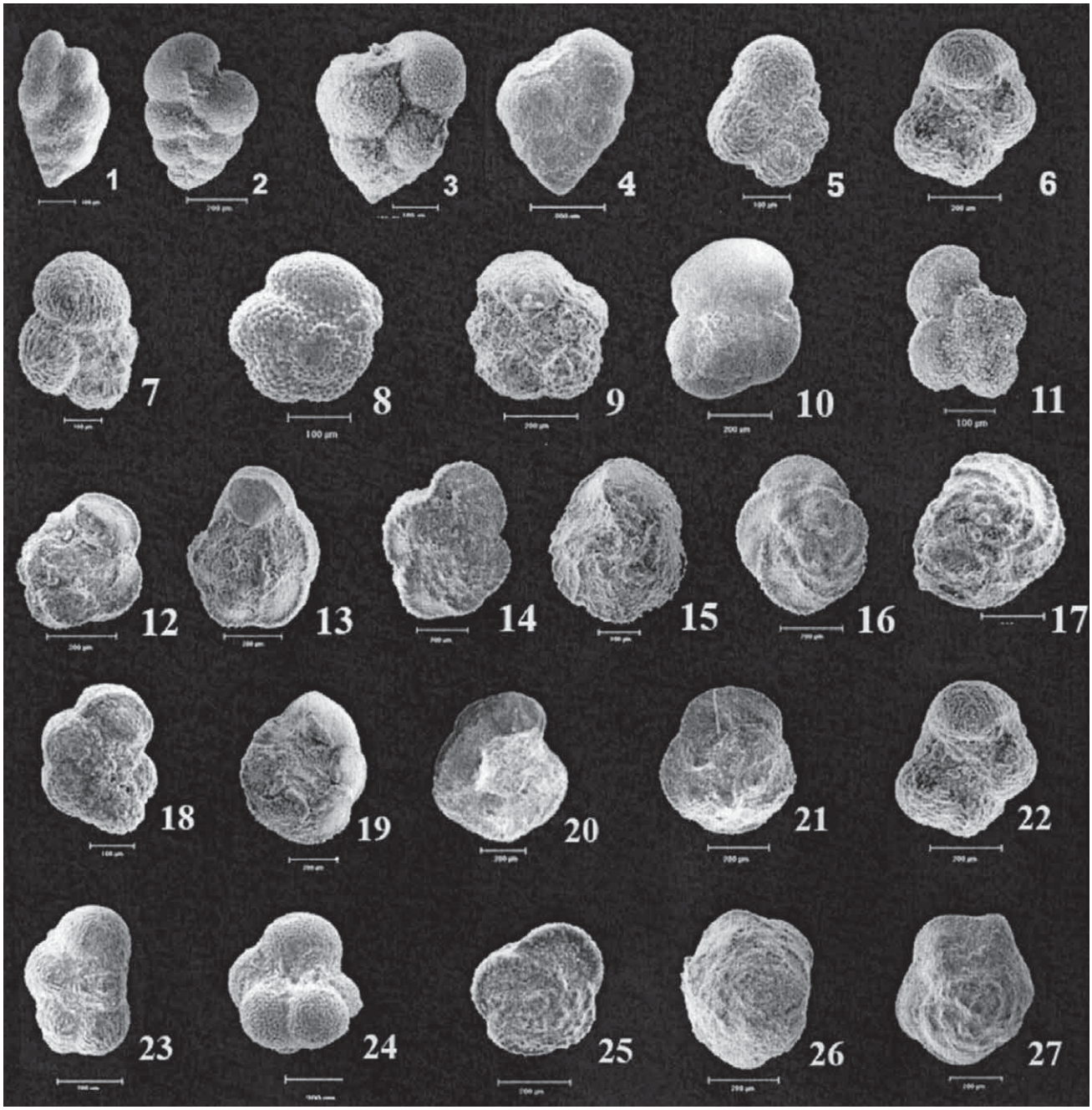

Figure 9: Planktonic Cretaceous plate. **1** – *Heterohelix navarroensis* (LOEBLICH, 1951); 4320 ft, Karama-3x. **2,3** – *Heterohelix globulosa* (EHRENBERG, 1840); 3630 ft, Karama-NW-5x. **4** – *Heterohelix* sp. 3810 ft, Karama-NW-5x. **5,6** – *Rugoglobigerina macrocephala* BRONNIMANN, 1952; 4320 ft, Karama-NW-1x. **7** – *Rugoglobigerina scotti* (BRONNIMANN, 1952); 4530 ft, Karama-NW-1x. **8** – *Rugoglobigerina* sp. 4770 ft, Karama-3x. **9** – *Rugoglobigerina rugosa* (PLUMMER, 1926); 3930 ft, Karama-3x. **10** – Globotruncanella sp. 3810 ft, Karama-NW-5x. **11** – Globotruncanella petaloidea (GANDOLFI, 1955); 4620 ft, Karama-E-1x. **12–14** – *Globotruncana linneiana* (D,ORBIGNY, 1839)); 4710 ft, Karama-3x. **15,16** – *Globotruncana* cf. *falsostuarti* SIGAL, 1952; 5520 ft, Karama-E-1x. **17,18** – *Globotruncana* sp. 4830 ft, Aqsa-1x. **19** – *Globotruncanita stuarti* (DE LAPPARENT, 1918); 4710 ft, Karama-3x. **20,21** – *Globotruncanita* cf. *stuartiformis* (DALBIEZ, 1955); 4770 ft, Karama-NW-5x. **22,23** – *Hedbergella* cf. *holdelensis* OLSSON, 1964; 4110 ft, Karama-3x. **24** – *Hedbergella delrioensis* (CARSEY, 1926); 4620 ft, Karama-3x. **25** – *Globotruncana* cf. *aegyptiaca* NAKKADY, 1950; 3930 ft, Karama-NW-X. **26** – *Rosita (contusotruncana) fornicata* (PLUMMER, 1931); 5940 ft, Aqsa-1x. **27** – Rosita (contusotruncana) contusa (CUSHMAN, 1926); 3780 ft, Karama-NW-1x.

Occurrence: Karama-E-1x (600–700 m), Karama-NW-1x (600–700 m), Karama-NW-5x (650–660 m) (in Apollonia Formation).

Remarks: In addition to the zonal markers, the nannofossil assemblage includes in the investigated wells the FO of both *Scyphosphaera magna* and *Ericsonia formosa* which define the base of NP12.

4.2.2.2. *Discoaster lodoensis* Zone (NP13)

Definition: LO of *Tribrachiatus orthostylus* or FO of *Toweius crassus* to the FO of *D. sublodoensis.*

Assemblage: The characteristic assemblage includes: *Coccolithus pelagicus*, *Ericsonia formosa, Helicosphaera lophota*, *Pontosphaera multipora*, *Sphenolithus moriformis*, *Pontosphaera multipora*, *Chiasmolithus solitus, Discoaster*

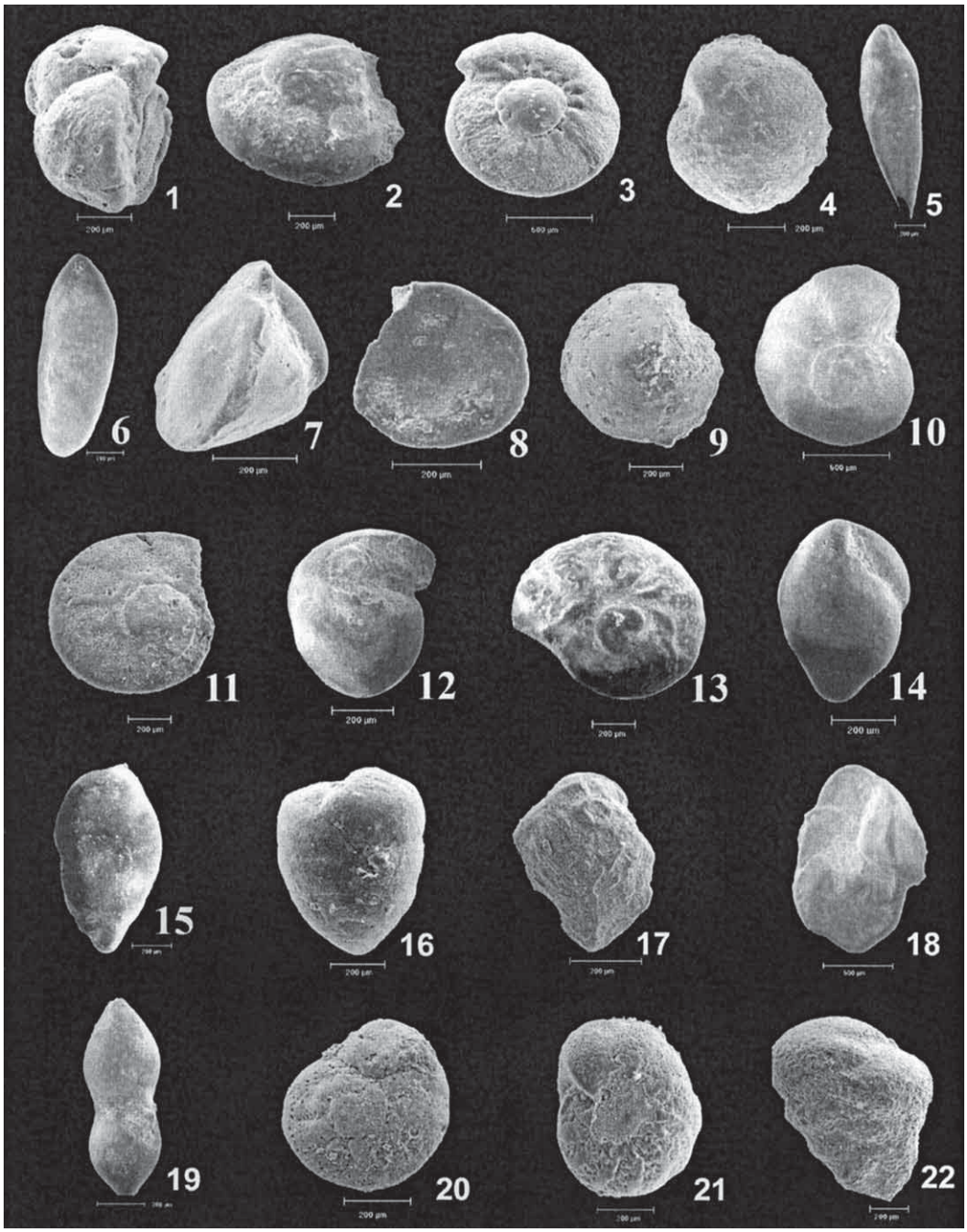

Figure 10: Benthic Cretaceous plate. **1** – *Gyroidinoides depressus* (HAGENOW); 3930 ft, Karama-NW-1x. **2,3** – *Gavelinella monterelensis* 4140 ft, Karama-NW-1x. **4** – *Stensioeina pommerana* BROTZEN; 4380 ft, Aqsa-1x. **5** – *Coryphostoma* cf. *gemma* CUSHMAN 1927; 4380 ft, Aqsa-1x. **6** – *Corphostoma crassum* VASILENKO, MYATLYUK 1947; **7–9** – Globorotalites conicus CARSEY 1926; 3780 ft, Karama-NW-1x. **10,11** – Cibicidoides sp.; 4470 ft, Karama-E-1x. **12** – *Gyroidina* sp.; 3990 ft, Karama-NW-5x. **13** – *Gavelinella* sp.; 3810 ft, Karama-NW-5x. **14,15** – *Arenobulimina* sp.; 4380 ft, Aqsa-1x. **16** – *Dorothia retusa* KAMIMSKI et al. 1988; 4710 ft, Karama-3x. **17** – *Bolivinoides draco* (MARSSON, 1878). **18** – *Cibicides* sp. **19** – *Laevidentalina* cf. *catenula* CUSHMAN &JARVIS 1932. **20,21** – *Anomalinoides* sp.; 4620 ft, Aqsa-1x. **22** – *Gaudryina Laevigata* FRANK 1914; 3990 ft, Karama-NW-5x.

barbadiensis, *Reticulofenestra dictyoda*, *Helicosphaera lophota*, and *Neococcolithes dubius.*

Authors: BRÖNNIMANN & STRADNER (1960) and BUKRY (1973)

Age: Early Eocene (Ypresian).

Occurrence: Karama-3x (800–1180 m)

Remarks: In addition to the zonal marker, the nannofossil assemblage includes (in the base of the zone) the FO of *Reticulofenestra dictyoda* and *Helicosphaera lophota.* Its top cannot be defined due to the marked hiatus which includes zones NP14 through NP17 in Karama-NW-5x.

4.2.2.3. *Discoaster tani nodifer* Zone (NP16)

Definition: This zone includes the stratigraphic interval from the LO of *Rhabdosphaera gladius* to the LO of *Chiasmolithus solitus.*

Assemblage: Besides the nominated species, Zone NP16 includes: *Ericsonia formosa, Helicosphaera lophota*,

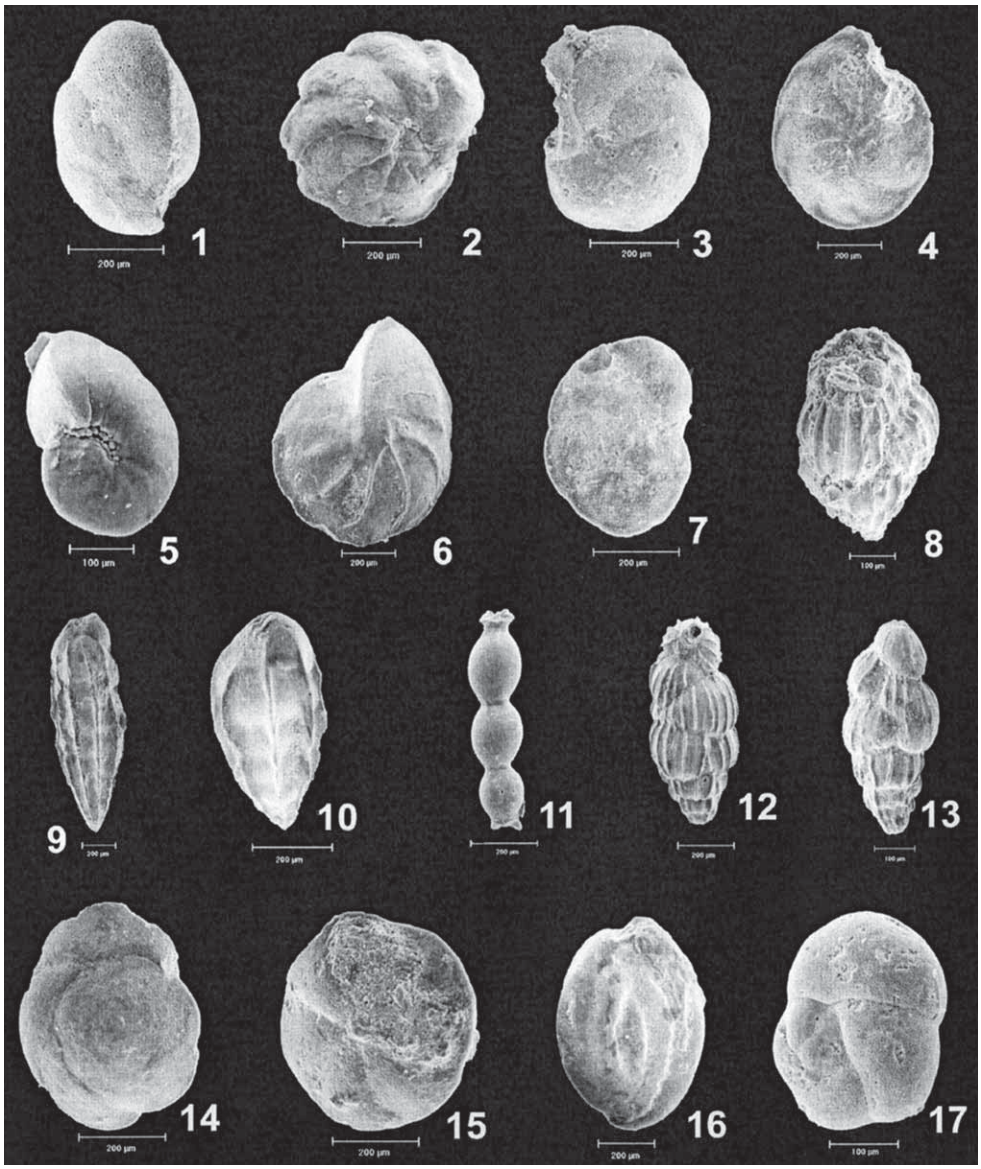

Figure 11: Benthic Eocene plate. **1** – *Cancris auriculus* FITCHTEL, MOLL, 1798; 1890 ft, Karama-NW-1x. **2** – *Hanzawaina* sp. 2100 ft, Aqsa-1x. **3** – *Cibicidoides ungerianus* 2130 ft, Karama-NW-5x. **4** – *Cibicidoides kullenbergi* PARKER, 1953; 2160 ft, Karama-3x. **5** – *Nonnion scaphum* FITCHTEL, MOLL, 1798; 1950 ft, Karama-3x. **6** – *Lenticulina* sp.1530 ft, Karama-3x. **7** – *Planulina* sp. 1800 ft, Aqsa-1x. **8** – *Uvigerina eocaena* GUMBEL, 1868; 1650 ft, Aqsa-1x. **9** – *Bulimina jacksonensis* CUSHMAN, 1925; 1800 ft, Aqsa-1x. **10** – *Bulimina alazanensis* CUSHMAN, 1927; 1890 ft, Karama-NW-1x. **11** – *Nodosaria* sp. 1890 ft, Karama-3x. **12,13** – *Uvigerina tempoalae* BOERSMA, 1984; 1740 ft, Karama-NW-1x. **14,15** – *Eponides ellisoare* SEGUENZA, EMEND, 1968; 1830 ft, Karama-E-1x. **16** – *Quinqueloculina seminula* LINNE, 1958; 1620 ft, Karama-E-1x. **17** – *Baggina* sp. 2430 ft, Karama-E-1x.

Pontosphaera multipora, *Sphenolithus moriformis*, *Pontosphaera multipora, Chiasmolithus solitus*, *Discoaster barbadiensis*, *Reticulofene stradictyoda*, *Neococcolithes dubius, Reticulofenestra hampdenensis*, *Cribrocentrum reticulatum, Sphenolithus moriformis*, and *Reticulofenestra umbilica*.

Authors: HAY et al. (1967), emend MARTINI (1970)

Age: Middle Eocene

Occurrence: Karama-NW-1x (705–760 m), Aqsa-1x (805–1080 m), Karama-3x (810– 1180 m) (in the Apollonia Formation).

Remarks: The base of the zone is placed at the level of the first appearance of *Reticulofenestra umbilica* in the studied wells. *Rhabdosphaera gladius*, the marker of the base of the zone is often of little use for zonation (PERCH-NIELSEN, 1985, p. 439). It is well known that *Reticulofenestra umbilica* has its FO at the base of the middle Eocene zone NP16 (MARTINI, 1971) and CP14 (OKADA & BUKRY, 1980).

In the study wells, a large scale hiatus is recorded below and above the sediments of Zone NP16, and thus the top and base of Zone NP16 cannot be accurately detected in such wells.

4.2.2.4. *Chiasmolithus oamaruensis* Zone (NP18)

Definition: This zone is defined as the interval from the FO of *Chiasmolithus oamaruensis* to the FO of *Isthmolithus recurvus*.

Assemblage: The zone includes the following nannofossil taxa:*,Pemma basquensis, Discoaster tanii, Pemma pa-*

pillatum, Reticulofenestra hillae, Cribrocentrum reticulatum, Reticulofenestra umbilica, Helicosphaera compacta, Discoaster tanii,Discoaster tanii nodifer, Ericsonia formosa, Reticulofenestra dictyoda, Reticulofenestra hampdenensis, Reticulofenestra hillae and Chiasmolithus oamaruensis.

Authors: MARTINI (1970)

Age: Middle to Late Eocene.

Occurrence: Karama-NW-5x, Aqsa-1x (560–1400 m), Karama-3x (660–740 m), Karama-E-1x (795–1250 m) (in Apollonia Formation).

Remarks: The base and top of Zone NP18 are well defined in Karama-3x, Karama-E-1x and Karama-NW-5x.

4.2.2.5. *Isthmolithus recurvus* Zone (NP19/20)

Definition: The interval from the first occurrence of *Isthmolithus recurvus* to the last occurrence of *Discoaster saipanensis,*and /or *Discoaster barbadiensis.*

Assemblage: Zone NP19-20 includes *Isthmolithus recurvus*, *Pemma basquensis*, *Reticulofenestra dictyoda*, *Discoaster tanii, Reticulofenestra hampdenensis*, *Reticulofenestra hillae,Cribrocentrum reticulatum, Sphenolithus moriformis*, and *Reticulofenestra umbilica.*

Authors: HAY, MOHLER & WADE (1966), EMENDED MARTINI (1970).

Age: Late Eocene.

Occurrence: Karama-3x (570–595 m), Karama-E-1x (630–700 m), Karama-NW-1x (620–705 m), Karama-NW-5x (650–680 m) (in Apollonia Formation).

Remarks: The first occurrence of *Isthmolithus recurvus* marks the base of the combined zone NP19/20. MARTINI (1971) used the lowest occurrence of *Sphenolithus pseudoradians* to define the base of zone NP20, but subsequent work (MARTINI, 1976) has shown that *S. pseudoradians* occurs much earlier and that the two zones cannot be differentiated. Therefore, zones NP19 and NP20 are also combined here, and Zone NP19/20 is defined as the interval between the first occurrences of *I. recurvus* and the last occurrence of *Discoaster saipanensis* and *D. barbadiensis*.

Figures 12 to 16 show the distribution of the nannoplankton in the different wells and some stratigraphically important taxa are represented in Figures 17 and 18 which are identified from the Aqsa-1x, Karama-3x, Karama-E-1x, Karama-NW-1x and Karama-NW-5x wells respectively.

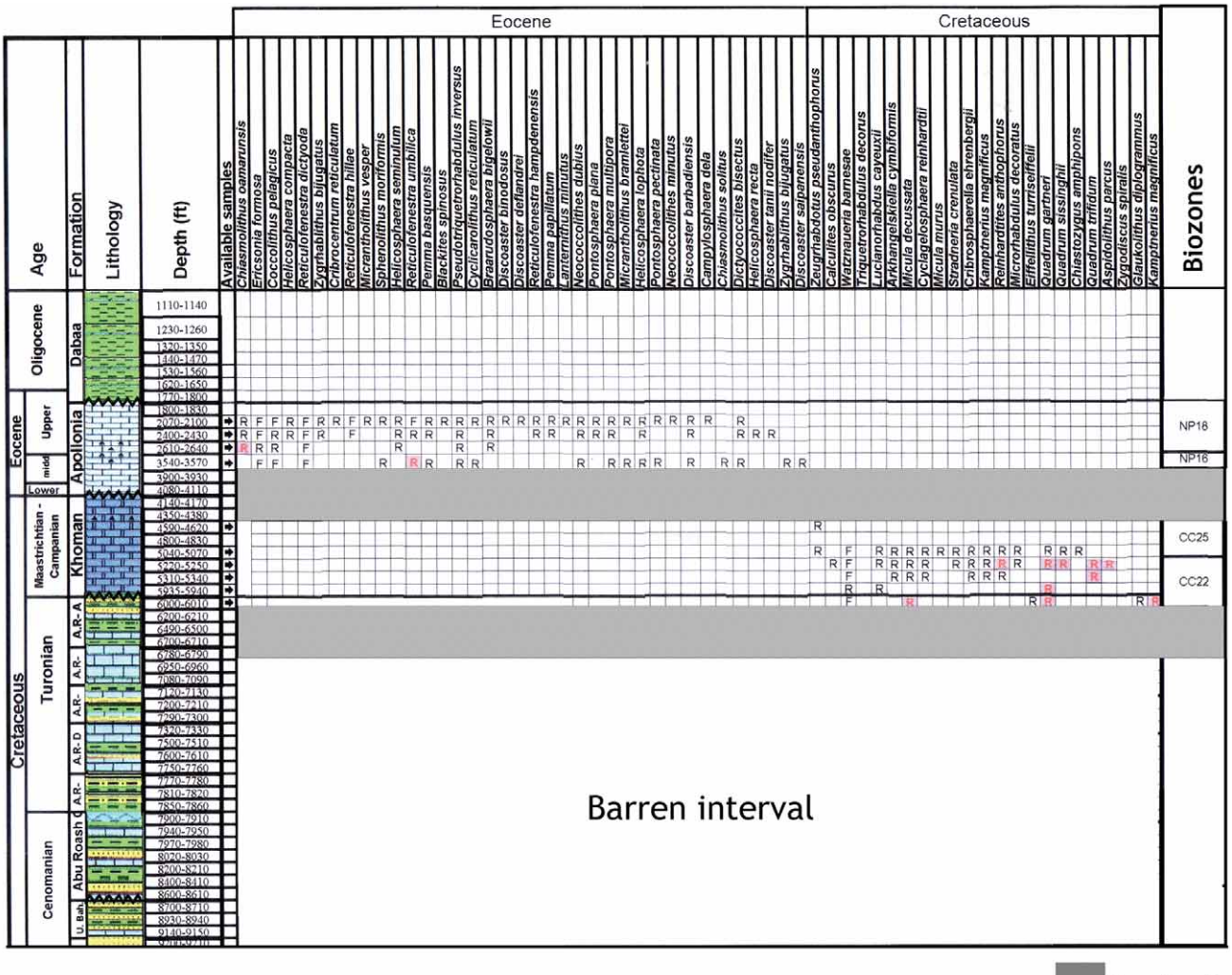

Figure 12: Distribution chart of the nannofossils of the Well Aqsa-1x.

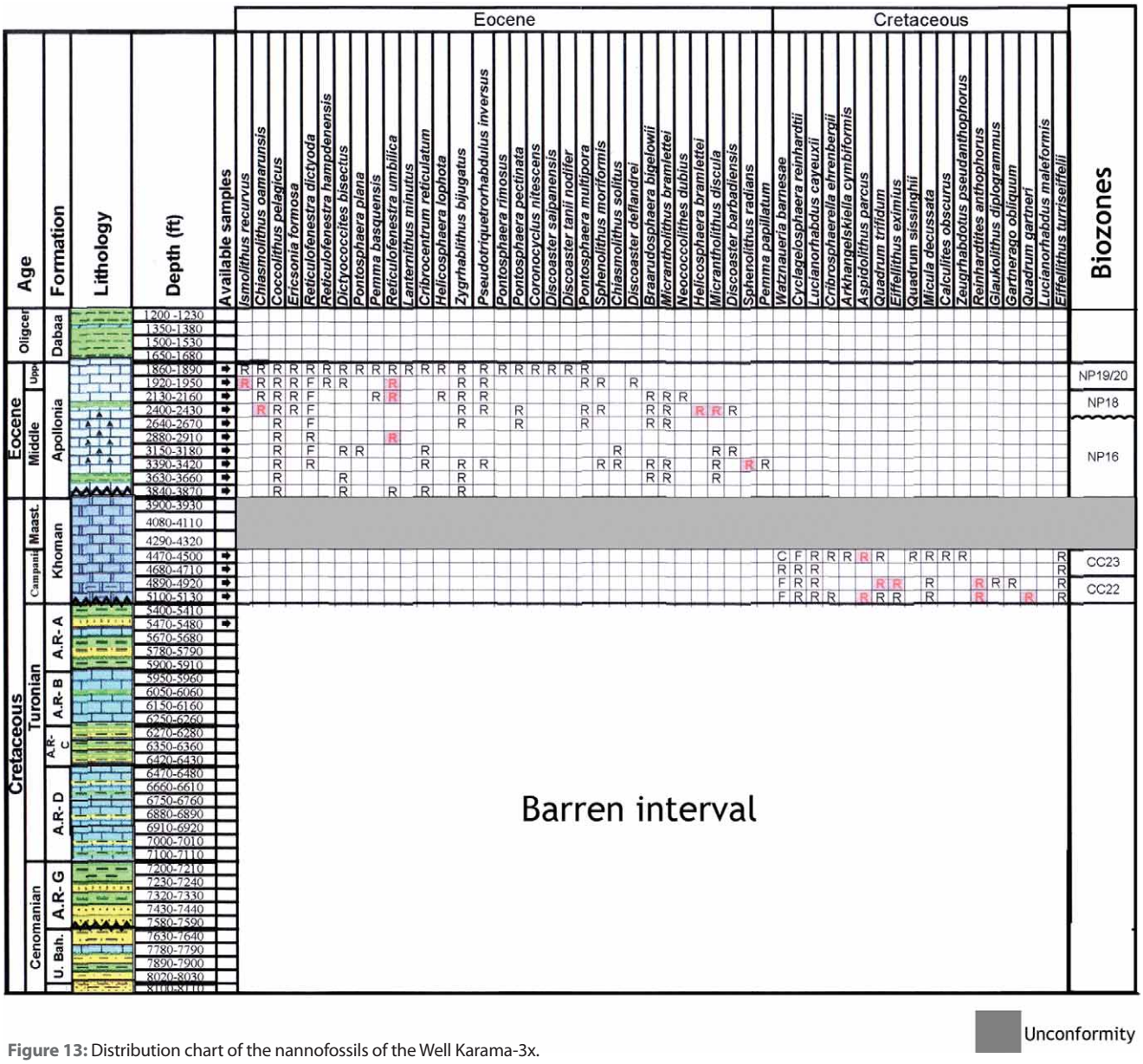

Figure 13: Distribution chart of the nannofossils of the Well Karama-3x.

5. SEQUENCE STRATIGRAPHY

The target of seismic stratigraphic analysis is to divide the seismic sections of the East Bahariya Concession into distinct depositional sequences that make up the investigated Late Cretaceous-Eocene succession in the study area. These sequences are bounded from above and below by marked sequence boundaries (EMERY & MYERS, 1996). The following steps were followed to achieve the aim of this study: A) Reorganization of the time-depositional units depending on the detected unconformities or changes in seismic patterns. B) Following these recognized unconformities in the different investigated seismic sections, it was important to define the major sequence boundaries. C) Seismic facies analysis, interpreting depositional environments from seismic reflection characteristics. D) Sequence stratigraphic analysis of the different formations using the available biostratigraphic data and lithological composition.

5.1. Detailed sequence stratigraphic analysis

Analysis of the sequence stratigraphy in the studied area is based mainly on the interpretation of various key surfaces (sequence boundaries (SB), transgressive surfaces (TS), transgressive surfaces of erosion (TSE) and maximum flooding surfaces (MFS)) and system tracts (lowstand systems tracts (LST), transgressive systems tracts (TST), highstand systems tracts (HST)) well logs (natural, radioactivity, receptivity and density logs) and foraminiferal content. These factors detect the depth and the environmental conditions during deposition in the seven investigated wells (AQSA-1X, AQSA-2x, KARAMA-3X, KARAMA-E-X, KARAMA-NW-1X, KARAMA-NW-5X, KARAMA-SW-1X and KARAMA-SW-10X) located in the studied East Bahariya concession (Figure 1).

The studied Upper Cretaceous-Eocene succession in the East Bahariya concession at the Western Desert is subdivided into five major 2nd order depositional sequences (UCS1,

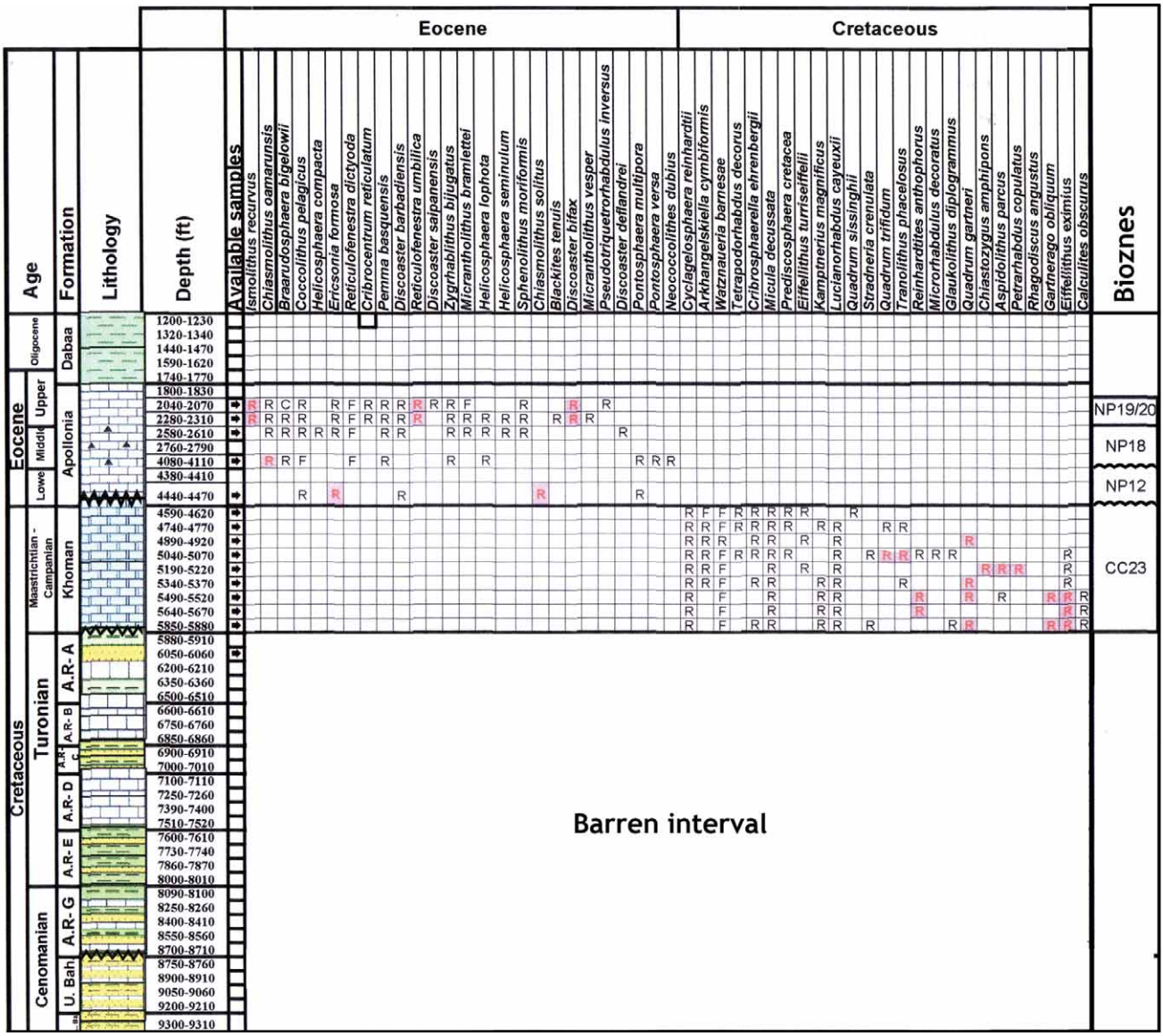

Figure 14: Distribution chart of the nannofossils of the Well Karama-E-1X.

UCS2, UCS3, ES and ORS). These are separated by four major depositional sequence boundaries (SB1, SB2, SB3 and SB4) as shown in (Figs. 19 and 20).

5.1.1. Upper Cretaceous sequence 1 (UCS1) (Cenomanian)

The first sequence (UCS1) is represented by the Upper Cretaceous rocks including the Upper Bahariya Fm. (Fig. 19). The top of this sequence is bounded by the depositional sequence boundary SB1 which represents the boundary between the Abu Roash-G Member and the underlying Bahariya Fm. It is the deepest identified and selected surface in the study area, which regionally, extends along the East Bahariya Concession, indicating a regional unconformity between the Abu Roash Formation and the underlying Bahariya Formation and the second order depositional sequence boundary (EL BASSYOUNY, 1970, CATUNEANU et al., 2006).

The base of this sequence can not be followed on the seismic sections because these are badly processed (Fig. 21), while the upper part of the Bahariya Fm. displays discontinuous, moderate to low amplitude reflectors. Internal configurations including onlap, toplap, downlap and parallel reflectors were recognized.

The external form of this sedimentary body appears either as sheet-like or wedge-shaped units. The principal internal configurations appear to be parallel to subparallel.

Interpretation

Clear differences between the high and low to moderate amplitude reflectors in this formation testify to the existence of at least two different lithological units. One has high amplitude and displays parallel to divergent reflector terminations. These units are interpreted as shale to siltstone beds. The other lithological units which have a low to moderate amplitude and are characterized by disconnected reflectors are interpreted as sandstone beds. According to Darwish et al., (1994) and ISMAIL et al. (1989) the Bahariya Formation lithologically is subdivided into the lower Bahariya and upper Bahariya units.

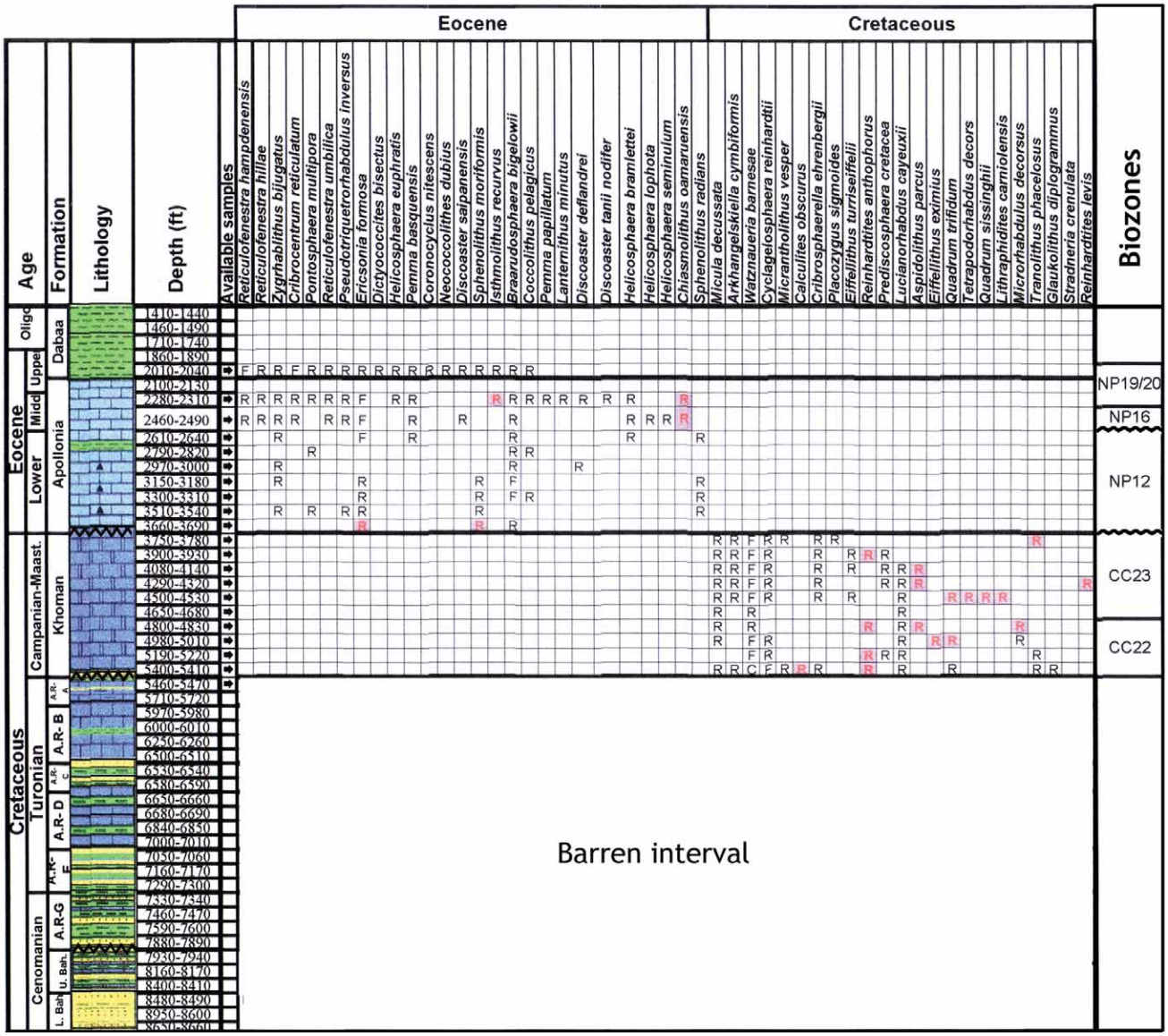

Figure 15: Distribution chart of the nannofossils of the Well Karama-NW-1X.

The Lower Bahariya Formation is composed of a relatively sand rich succession of fine to medium grained sandstone and shale while the Upper Bahariya Formation is composed mainly of very fine-grained sandstone with shale intercalated with limestone beds. Pyrite and glauconite minerals are common, which were deposited in a shallow marine to fluvio-marine environment with alternating high and low energy.

Based on the results of the analyzed seismic lines, this subdivision of the Bahariya Fm. into two units has been identified in the all investigated seismic lines thus confirming the interpretation of the seismic facies.

5.1.2. Upper Cretaceous sequence 2 (UCS2) (Cenomanian–Turonian)

5.1.2.1. Abu Roash-G Member (Cenomanian)

Based on the interpretation of the seismic lines, the Abu Roash-G Member can be subdivided into two main parts. The lower part is characterized by low amplitude and moderate continuity reflectors. Their reflection geometry at the sequence boundaries is considered as erosional truncation (Fig. 23).

From the studied seismic lines the reflection geometry at the sequence boundaries are considered concordant with lower and upper sequence boundaries of this formation. The seismic facies of the lower part of the Abu Roash-G Member appears as low to moderate amplitude and moderate continuous reflectors in the internal configuration as parallel reflectors, which in the external outline seems to represent elongated wedge-shaped beds.

The seismic facies of the upper part of the Abu Roash-G Member is characterized by high amplitude and very continuous reflectors. The internal reflection geometry at the upper sequence boundary is considered concordant and runs parallel to the sequence boundary (Figs. 21 and 23).

Interpretation

The characteristic configuration of the seismic facies in the lower part of the Abu Roash-G Member is interpreted as sand

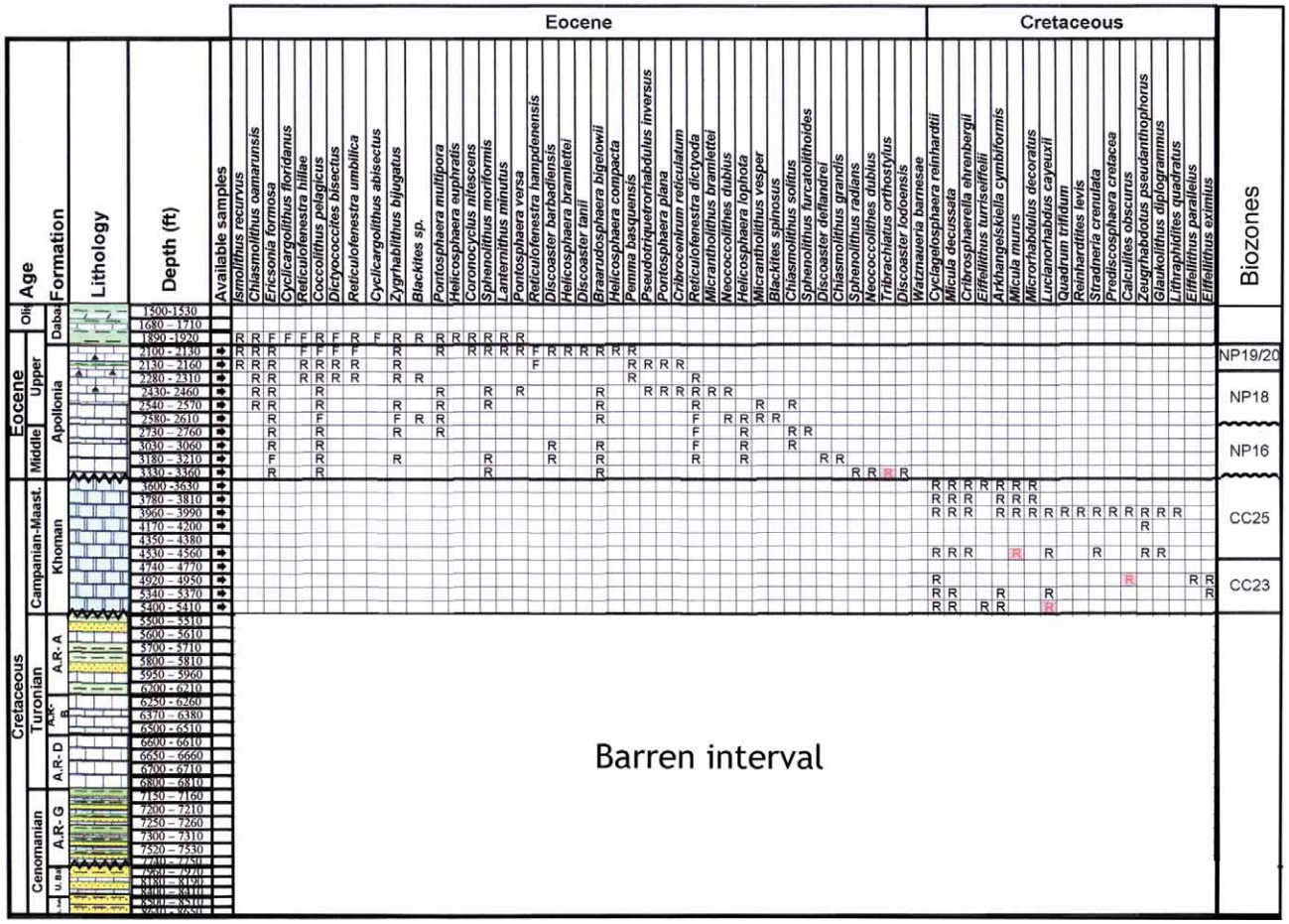

Figure 16: Distribution chart of the nannofossils of the Well Karama-NW-5x.

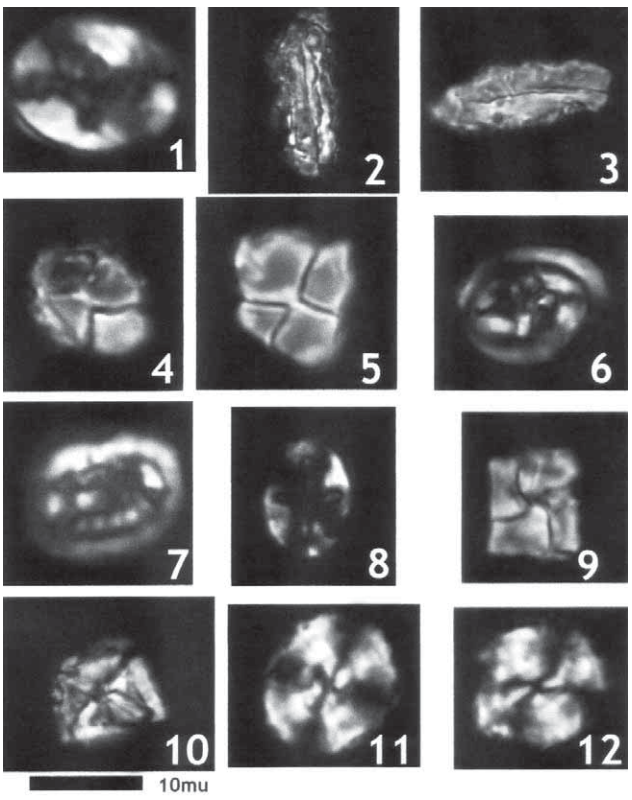

bars (Fig. 23). The low amplitude and discontinuity of the seismic reflectors support this interpretation. These sand beds may represent deposits of a prograding delta system, with offshore (pro-delta) silty mudstones at the base overlain by (in ascending order) lower, middle and upper shoreface sandstone, distributary-mouth bar sandstone.

The internal configuration as parallel reflectors of the upper part is interpreted as homogenous sediments, which are arranged in parallel thin beds. These features exhibit cycles of mudstone, glauconitic siltstone, limestone, and sandstone deposits.

Based on the depositional environment of the Abu Roash-G Member (MARK et al., 2009) which is considered

Figure 17: Nannofossils Cretaceous plate. **1** – *Eiffellithus turriseiffelii* (DEFLANDRE in DEFLANDRE & FERT, 1954) REINHARDT (1965) K-NW-1x; **2,3** – *Lucianorhabdus cayeuxii* DELANDRE (1959), depth (5040-5070) Aqsa-1x; **4,5** – *Calculites obscurus* (DEFLANDRE, 1959), depth (4470-4500) K-3X; **6** – *Reinhardtites anthophorus* (DEFLANDRE, 1959), depth (5640-5670) K-E-1X; **7** – *Cribrosphaerella ehrenbergii* (ARKHANGELSKY, 1912), depth (5100-5130) K-NW-1X; **8** – *Eiffellithus eximius* (STOVER, 1966) depth (5850– 5880) K-E-1X; **9,10** – *Micula murus* MARTINI (1961), depth (4470–4500) K-3X; **11,12** – *Watznaueria barnesae* (BLACK in BLACK & BARNES, 1959), depth (5935–5940) Aqsa-1x.

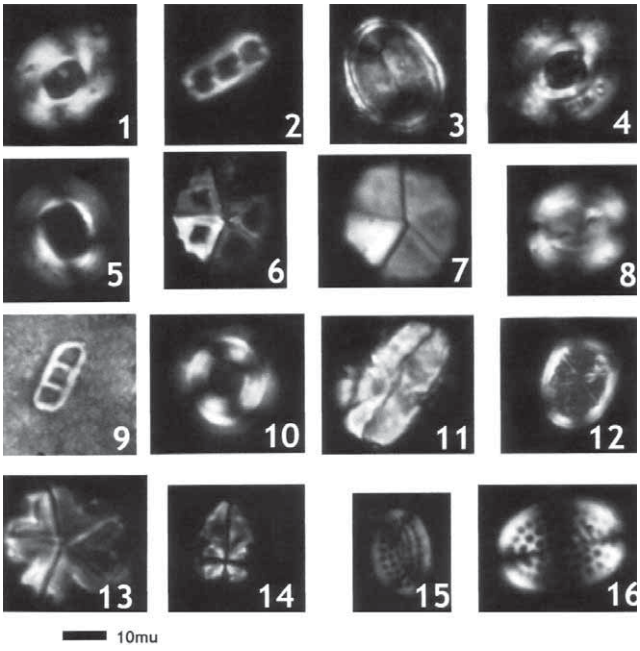

Figure 18: Nannofossils Paleogen plate. **1** – *Reticulofenestra hillae* BUKRY & PERCIVAL (1971) Aqsa-1x; **2** – *Ismolithus recurvus* DEFLANDRE (1959), depth (1920–1950) K-3x; **3** – *Pemma basquensis* (MARTINI, 1959c) BALDI-BEKE (1971) K-NW-1x; **4** – *Reticulofenestra umbilica* (LEVIN, 1965), depth (2400–2430) Aqsa-1x; **5** – *Pontosphaera multipora* (KAMPTNER, 1948) ROTH (1970) K-NW-1x; **6** –*Blsmolithus recurvus* DEFLANDRE 1959 K-E-1x; **7** – *Braarudosphaera bigelowii* (GRAN & BRAARUD, 1935), depth (2130–2160) K-3x; **8** – *Dictyococcites bisectus* (HAY, MOHLER, WADE, 1966), depth (1920–1950) K-3x; **9** – *Ismolithus recurvus* DEFLANDRE (1959), depth (1920–1950) K-3x; **10** – *Ericsonia formosa* (KAMPTNER, 1963), depth (2400–2430) K-NW-5x; **11** – *Zygrhablithus bijugatus* (DEFLANDRE in DEFLANDRE & FERT, 1954), depth (2640–2670) K-3x; **12** – *Chiasmolithus oamarunsis* (DELLANDRE, 1959), depth (2400–2430) K-3x; **13** – *Micrantholithus bramlettei* (BRONNIMANN & STRADNER, 1960), depth (3390–3420) K-3x; **14** – *Sphenolithus radians* DEFLANDRE in GRASSE (1952), depth (3390–3420) K-3x; **15,16** – *Pontosphaera multipora* (KAMPTNER, 1948), depth (2400–2430) K-3x.

to be delta to shallow marine environment, our interpretation agrees with the statements and characteristic features such as sandstones bodies and shale beds that were recognized in the interpreted seismic lines (Figs. 21, 23 and 24).

5.1.3. Abu Roash A, B, C, D, E and F members (Turonian)

The Abu Roash Fm. is generally characterized by several strong correlated internal reflectors representing the contacts between its members. The parallel reflectors alternate with weak to moderate internal reflectors, which show chaotic to hummocky internal configurations (Fig. 24). The external forms of these members (A, B, C, D, E and F) display different geometries such as sheet-like and wedge-shaped forms, which can be indicated by parallel to divergent internal reflection configuration.

Based on Biostratigraphy BARAKAT et al. (1987), these facies features exhibit cycles of shallow marine limestone, sandy limestone and shale of the Abu Roash **A**, shallow of the Abu Roash **B** Member, relatively restricted deep marine shale, sandstone and limestone of the Abu Roash **C** Member, the limestone and shale of Abu Roash **D**, shallow marine

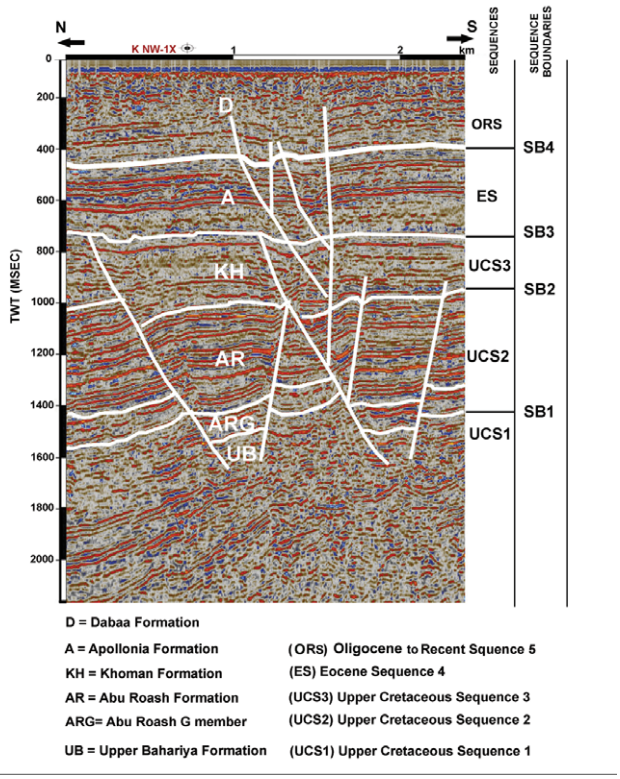

Figure 19: An interpretation of seismic section 5455.

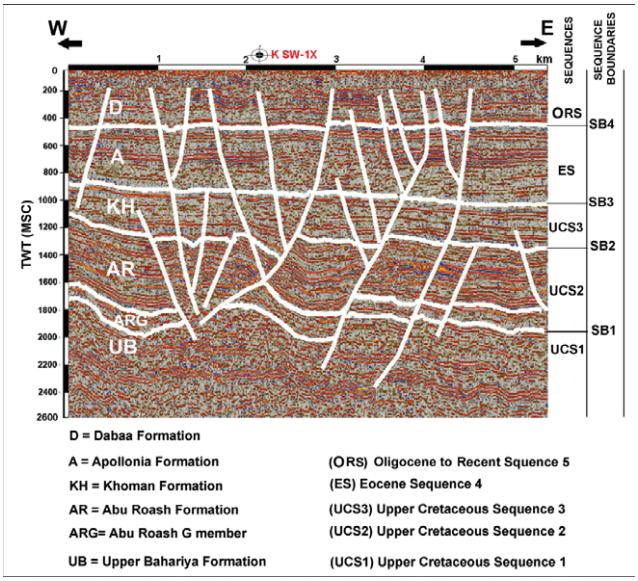

Figure 20: An interpretation of seismic section 1417.

sand and shale of the Abu Roash **E** Member, and the deep marine limestone and shale of the Abu Roash **F** Member (Figs. 23 and 25).

Interpretation

The alternation between weak –moderate and high amplitude internal reflectors suggests at least two different lithological units. The obvious parallel reflectors are interpreted as shale beds. The low amplitude reflectors have a chaotic to hummocky internal configurations, which indicate impure lime-

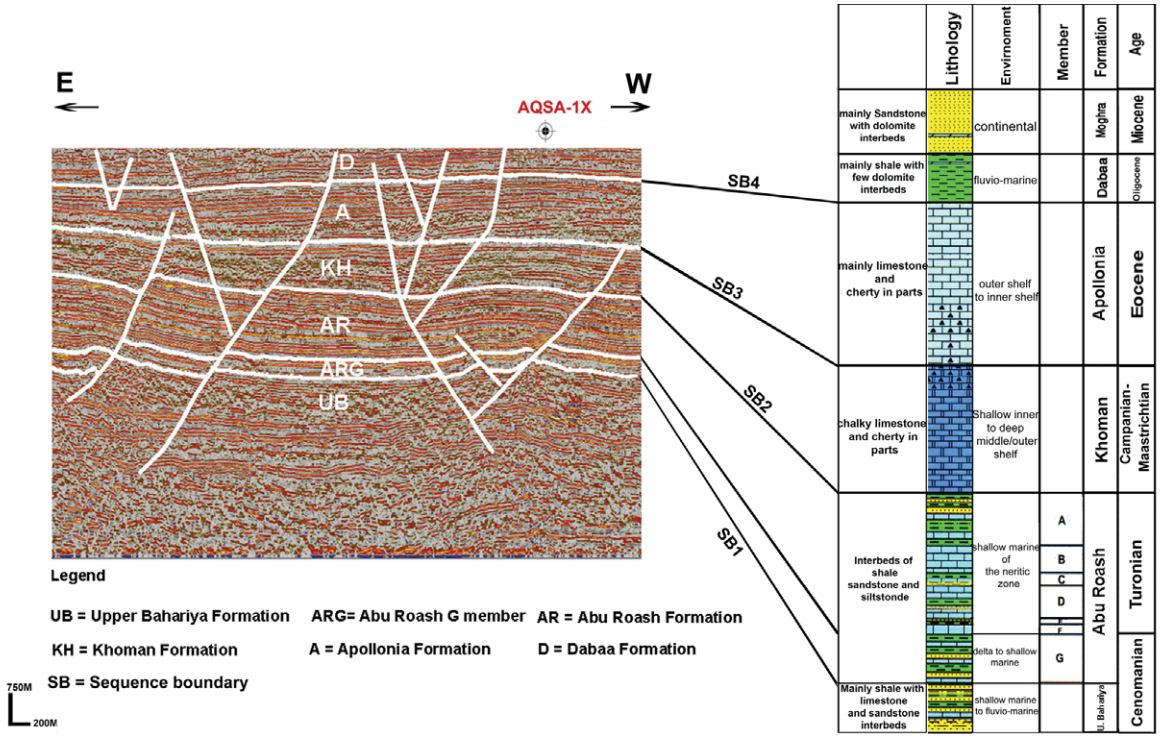

Figure 21: Lithologic section of the Upper Cretaceous-Eocene Succession correlated with seismic profile 1219.

stone or highly bioturbated sandstone beds. The Abu Roash Fm. of Turonian age consists of limestone with shales and sandstone intercalations providing a good source reservoir and cap rocks for hydrocarbons (BAYOUMI et al., 1987).

According to BARAKAT (1987) the habitats of the faunal assemblage together with the occurrence of detrital quartz grains in the Abu Roash F-A Members suggest a shallow marine environment of the neritic zone. Furthermore the Abu Roash Fm. was deposited in shallow-shelf to open-marine conditions (BARAKAT et al**.,** 1987; BAYOUMI et al., 1994, 1996).

5.1.4. Upper Cretaceous Sequence 3 (UCS3) (Campanian-Maastrichtian)

The Khoman Fm. is equivalent to sequence (UCS3). This sequence is bounded by SB2 below and the above. SB2 is at the end of the Turonian. Detailed analysis of SB2 reveals that it is of the type 2 boundary of VAN WAGONER et al. (1988). It is characterized by partial erosion of the Coniacian and Santonian between the Khoman and the top of the Abu Roash Formation, as shown by truncation of the top Abu Roash especially in structurally uplifted places (BAYOUMI & LOTFY, 1989). It is an important disconformity recorded in all the Cretaceous-Tertiary successions of Egypt (HEWAIDY et al., 2006).

The seismic facies of the lower part of the Khoman Fm. is moderate to low in the continuity and amplitude represented by disconnected refractors. These reflectors exhibit several characteristic terminations such as onlap, truncations and complicated sigmoidal configurations. A group of parallel irregular reflectors is characteristic for this lower part of the Khoman Fm.

The seismic facies of the middle part of the Khoman Fm. is entirely different in character which is dominated by very weak continuity and amplitude with prevailing chaotic seismic configurations (Fig. 26). The external geometry of this part represents an inhomogeneous lithological character, which appears to be similar to reef or salt dome geometry (Fig. 26).

The internal configuration of the upper part of the Khoman Formation is characterized by very high continuity and amplitude with parallel reflectors. These reflectors extend concordantly with the upper boundary of this sequence and display onlap and oblique parallel configurations. The external geometry in the upper part occurs as sheet like units to platform geometry especially to the north of the study area (Fig. 26).

Interpretation

Based on the fossil content and the description of the seismic facies with respect to characteristics of these seismic reflectors, one could conclude that the logical interpretation of the seismic configuration, such as very closed and parallel reflectors, indicate a well bedded and homogenous lithology, which can be shale beds intercalated with limestone or chalk.

Parallel, irregular reflectors groups are interpreted as isoclinals small folds within the lower part of the Khoman Fm. Fold structures can be attributed to compressional stress in the study area during the Late Cretaceous.

The poorly and weak amplitude reflectors in the middle part indicate massive chalk limestone. The moderate to low continuity and amplitude signify limestone with a high number content of chert nodules. This interpretation agrees with the lithology of the Khoman Fm. which consists mainly

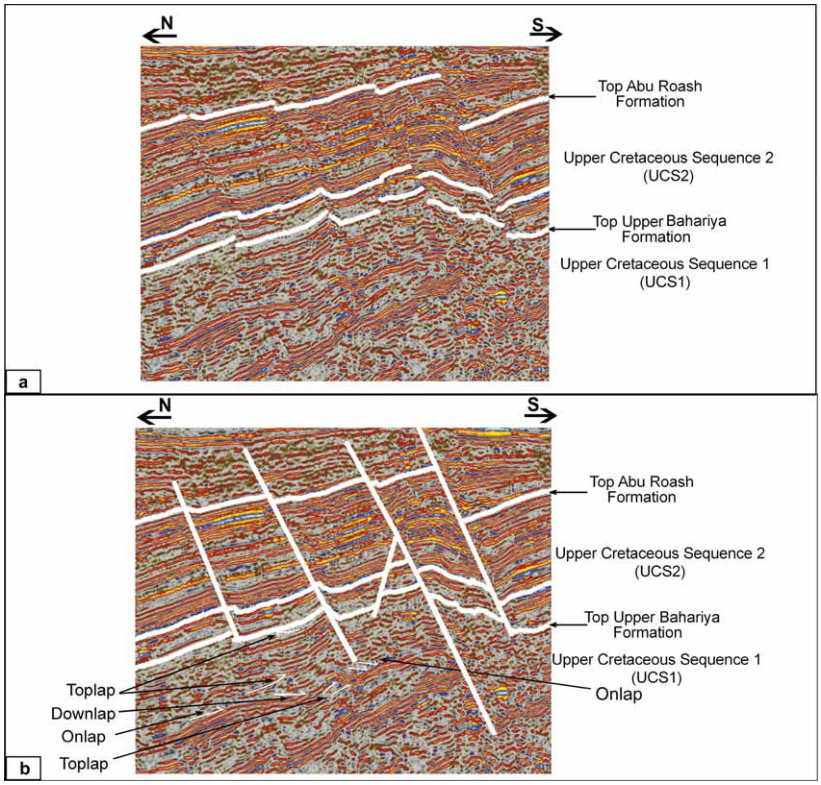

Figure 22: Shows the lower part of seismic line 5667(middle of the study area), (b): The interpreted seismic line 5667 displaying the main internal configurations which characterized the seismic facies of Upper Cretaceous Sequence 1 (UCS1).

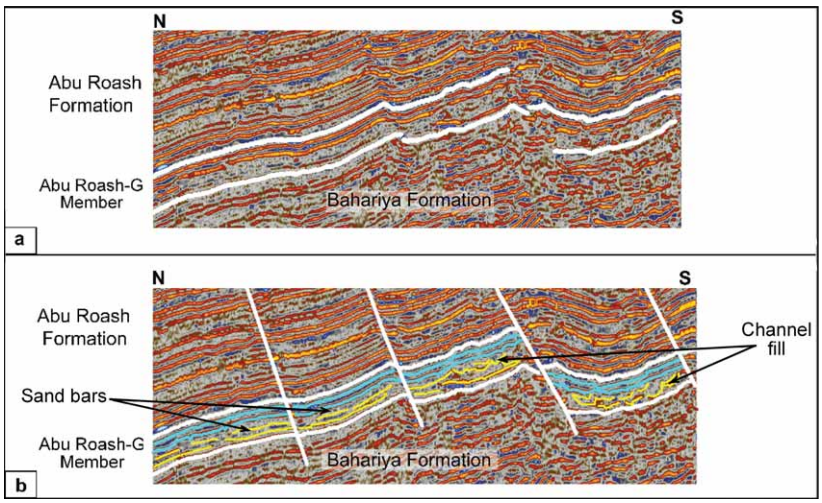

Figure 23: Shows the lower part of seismic line 5727(middle of the study area), (b): The interpreted seismic line 5775 illustrates the internal configurations of sandstone in the lower part of Abu Roash-G Member as a part of Upper Cretaceous Sequence 2 (UCS2).

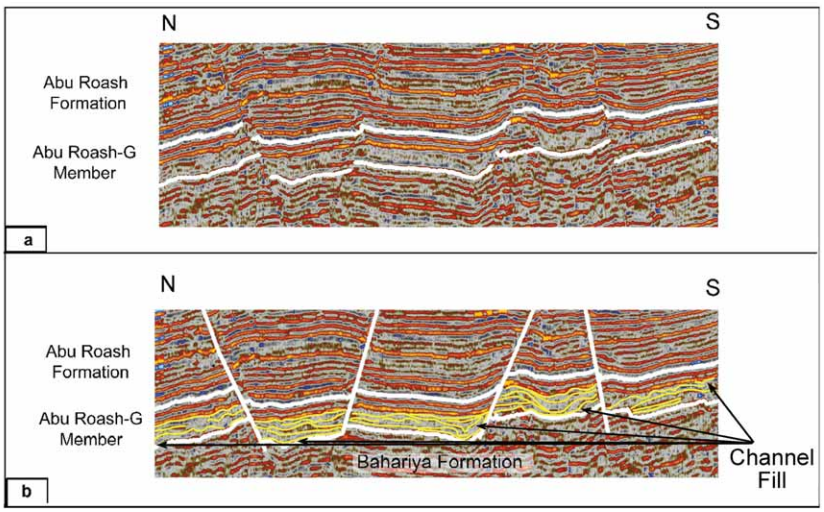

Figure 24: Showing the lower part of seismic line 5930 (east of the study area), (b): The interpreted seismic line 5930 illustrates the internal configurations of sandstone in the lower part of Abu Roash-G Member as a part of Upper Cretaceous Sequence 2 (UCS2).

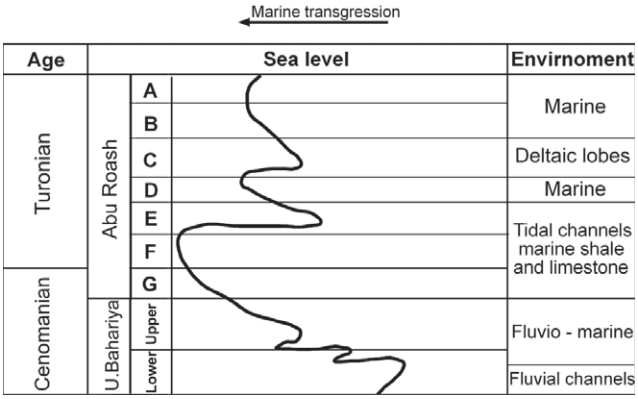

Figure 25: Relative sea level fluctuations in the Upper Cretaceous, Western Desert.

of chalky limestone with pyritic, cherty strata in the lower part and interbeds of shale in the upper part (BARAKAT et al., 1984, ABDEL HAMID, 1985 & GHANEM, 1985).

Facies characteristics, faunal content and planktonic ratio indicate an upward shallowing in the depositional regime from a deep middle/outer to shallow inner shelf during deposition of the Khoman Formation (HEWAIDY et al., 2006).

5.1.5. Eocene sequence 4 (ES)

The fourth sequence is represented by Eocene sediments (ES), which comprise the Apollonia Formation (Figs. 19, 20). This sequence is bounded by SB3 in the lower part and by SB4 at the upper part Figs. 19 & 20, show the SB3 which appears at the end of the Upper Cretaceous (Campanian – Maastrichtian) and separates between the Eocene sequence (ES) and Upper Cretaceous sequence (UCS3) sequences. The SB3 has moderate to high amplitude reflectors and is also marked by the radioactivity increase in the gamma ray logs (Fig. 27).

Based on the fossil content, the available data and former geological studies, the lower part of this sequence boundary is affected by submarine erosion causing the erosion causing the removal of the uppermost part of the Maastrichtian and all of the Palaeocene (BAYOUMI et al., 1987).

Seismic facies of this sequence which is represented by sediments of the Apollonia Formation have three main features which are also very clear in the gamma logs.

The seismic facies of the lower part of the Apollonia Fm. is moderate to low both in continuity and amplitude, while to the north of the area; reflectors are moderate to high amplitude and continuity. The internal configurations appear to be parallel to divergent (Fig. 28). This part shows the increase in gamma rays (more than the upper part of the Khoman Formation). In general the reflection geometry at the lower sequence boundary of the Apollonia sequence is considered concordant and exhibits even onlap near to central part of the study area (Fig. 28)

The seismic facies of the middle part of the Apollonia Formation is distinguished by high continuity and amplitude. Also the principal internal configurations appear to be parallel to the divergent reflectors. The external form of these sediments is considered to be a wedge like geometry with local irregular bedding features. These structures occur as small isolated and relative high amplitude reflectors of small domal structures.

The seismic facies of the upper part of the Apollonia Formation is characterized by low to moderate continuity and amplitude. The principal internal configurations appear to be parallel to divergent. The external form of these sediments is sheet-like and wedge shaped units.

The foraminiferal assemblage recorded from the upper part of this sequence suggests the end of the restricted environment that prevailed during deposition of the underlying Eocene sediments.

Interpretation

Based on the seismic facies configurations the parallel high amplitude reflectors display a carbonate ramp geometry, which has a very slight dip and occurs as an elongated wedge. The local irregular bedding structures are interpreted as convolute bedding which may be related to slumping.

This carbonate ramp extends from north to the south (Fig. 28). It is worth mentioning, that the thicknesses of this

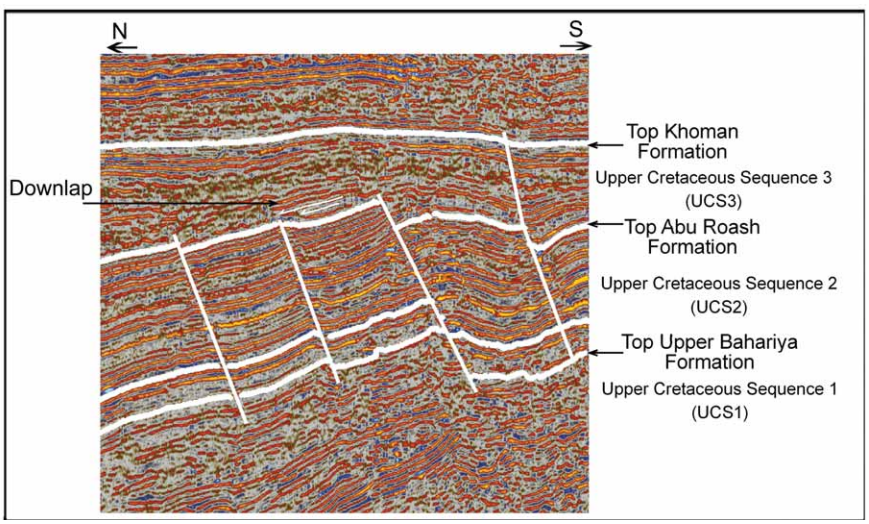

Figure 26: Showing one of the internal configuration which distinguish the seismic facies of Upper Cretaceous Sequence 3 (UCS3) (upper part of line 5667).

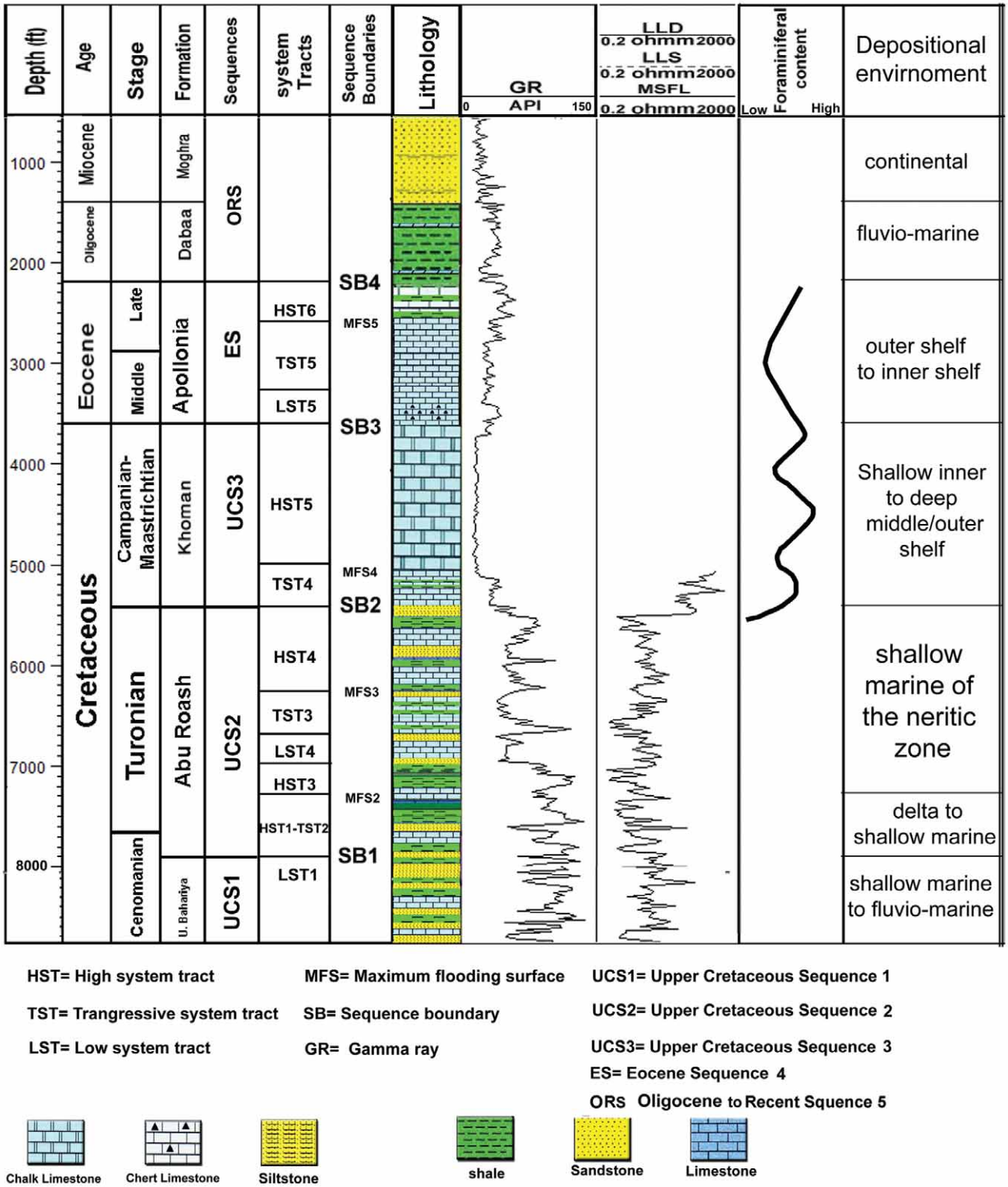

Figure 27: System tracts, logs, fauna and depositional environment of Well K-NW-1X.

carbonate ramp decreases laterally to the south. The low amplitude reflectors in the lower part indicate a heterogeneous lithology, which may be related to mixed pure carbonate sediments contaminated with cherty nodules and lenses parallel to bedding.

The lithological composition and the characteristics of the seismic reflectors of this sequence suggest that its depositional conditions range the inner shelf at the base to the outer shelf at the top of this sequence.

5.1.6. Oligocene to recent sequence 5 (ORS)

The Oligocene to recent facies in the study area are represented by the sediments of the Dabaa Fm. in the lower part and the Moghra Fm (Miocene) at the top of the investigated

seismic lines. Both formations build up a complete sequence the lower boundary of which is represented by the sequence boundary (SB4), whereas the upper boundary represents the top of all interpreted seismic lines in the study area. The sequence boundary represents the unconformity surface due to erosion of sandstone and siltstone from type section defined in the Dabaa-1 well (TAWADROS, 2001).

Based on the analyzed lines, the seismic facies of the Upper top facies are characterized by: Internal configuration of the lower part gradually increasing in both the continuity and frequency of seismic reflectors upward showing several seismic terminations such as toplap with parallel to sigmoidal configurations. These reflectors run parallel to each other and display a high amplitude and frequency in the middle part of this sequence. The external form of this unit resembles sheet-like units.

The upper part of the sequence is characterized by chaotic, discontinuous, high frequency and low amplitude reflectors (Fig. 29). The internal configuration of the seismic facies is characterized by seismic termination features: onlap, toplap and erosion truncations. The external form is of the sheet-like and wedge shaped units with observable channel-like geometry.

Interpretation

A gradually increase in both the continuity and frequency of the seismic reflectors in the lower part of this sequence indicates changes in the lithology. Hence the lower part of this sequence is interpreted as shale beds of the Dabaa Formation intercalated with evaporites concentrated in the lower part of the sequence and characterized by low amplitude reflectors and very chaotic seismic configuration (Fig. 29).

The upper part of this sequence is interpreted as sandstone beds of the Moghra Formation because of the relatively low seismic reflectors, in addition to the occurrence of typical sandstone features such as channel fill structures.

These characterize the Upper top facies of the Dabaa and Moghra Formations suggesting a change from shallow marine inner shelf environment at the base to fluvial facies at the top. This assumption agrees in some points with the interpretation of the seismic lines.

5.2. Gamma ray response

The change in the gamma ray responses in the various units can be recognized. The boundary between units **UCS1** and **UCS2** is marked by a decrease in the gamma ray values (Fig. 30).

The presence of sandstone and shale intercalations in many parts of the **UCS1** unit causes oscillation of the gamma ray curve (Figs. 29, 30). The contact between the units **UCS2** and **UCS3** can be detected by a decrease in the gamma ray values (Figs.20, 29) accompanied with the change from shale to limestone lithofacies.

The boundary between the unit **UCS3** and the **ES** is marked by a slight increase in the gamma ray values. **UCS3** shows no change in gamma ray values because it is composed only of chalk limestone. The **ES** unit shows some high values in the gamma ray log which are ascribed to the shale intercalations in this unit (Fig. 29).

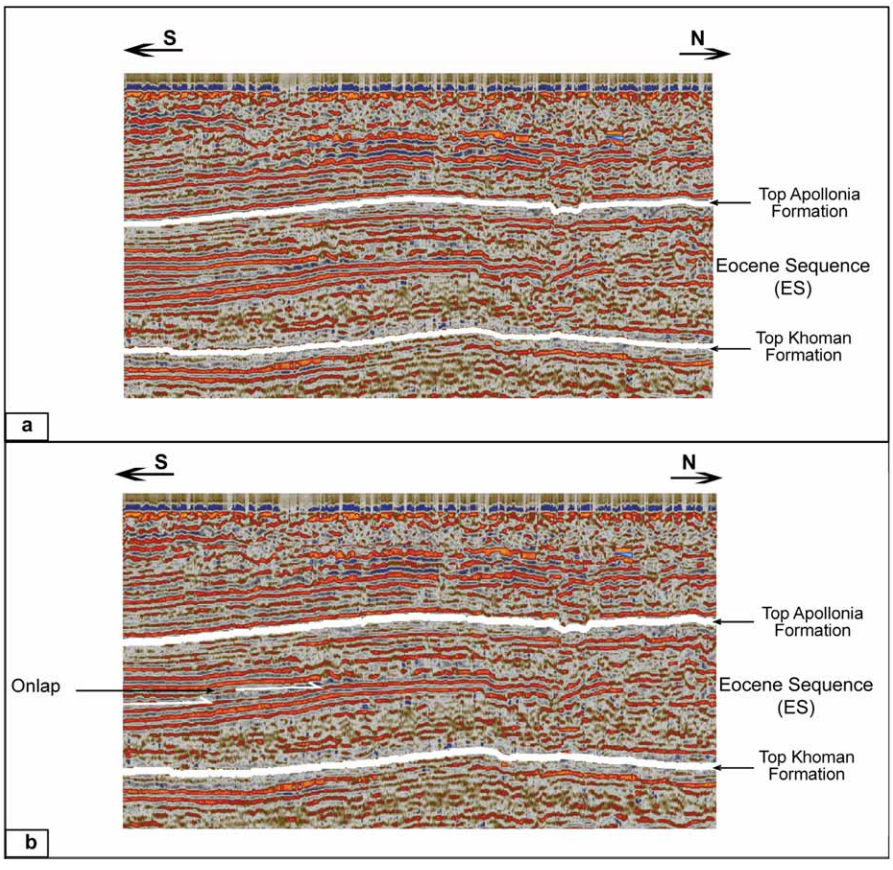

Figure 28: Showing the lower part of seismic line 5630 (middle of the study area), (b): The interpreted seismic line 5630 illustrating the internal configurations of Eocen Sequence.

The upper part of the **ORS** unit is characterized by a marked decrease in the gamma ray values with respect to the underlying unit **ES**.

6. DISCUSSION OF THE SYSTEMS TRACTS

The Upper Cretaceous – Palaeogene succession in the East Bahariya concession is divided into 17 systems tracts. These systems tracts are outlined below:

6.1. System tracts of Cenomanian age

6.1.1. Lowstand systems tract (LST1)

This systems tract represents the first one studied in this work. It comprises the upper part of the first sequence (UCS1), which represents the upper part of the Bahariya Formation. The lower boundary of this tract is not traceable on seismic profiles. This lowstand system is characterized by low GR and relatively high resistivity (Fig. 30).

Sediments of the LST1 are mainly sandstones with siltstone interbeds. These deposits are overlain by the clastic and non-clastics deposits of shale and limestones, which belong to the lower part of the Abu Roash-G Member (Fig. 31).

The available data indicate that this interval represents the maximum drop in sea level. This drop started with the deposition of the coarse clastics (sandstone) of the Bahariya Formation and continued and increased with deposition of more clastics and evaporites. This systems tract is widely recognized across the Western Desert.

The TST is missing, due to either non-deposition or subsequent erosion. The HST of this sequence is also missing, most likely due to subaerial erosion (fluvial incision) where the upper (LST1) is directly overlain by the 2nd order depositional sequence of the Abu Roash Formation, being truncated at the top by the sequence boundary (subaerial unconformity).

The age of this lowstand system is Early Cenomanian. The LST1 deposits are limited by the first sequence boundary (SB1), which delineates the end of the 1st sequence and the beginning of the second.

6.1.2. Highstand systems tract 1 (HST1)

Based on the available data and their resulting interpretations LST and TST system tracts in the investigated well sections are entirely missing. The absence of these may be attributed to the erosion cycle, which is indicated by truncation at the top by the sequence boundary due to subaerial unconformity.

This highstand system tract occurs in the Lower part of the Abu Roash-G Member, and represents the maximum phase of transgression after deposition of the Bahariya Formation (Fig.32).

The progradational HST1 sediments are characterized by an upward increase in GR and moderate to low resistivity. Lithofacies of the HST1 sediments are entirely different from those of the LST1 sediments (Fig. 31), and includes mainly shales and limestones. The limestone is laterally variable in thickness whereas the shale is concentrated mainly

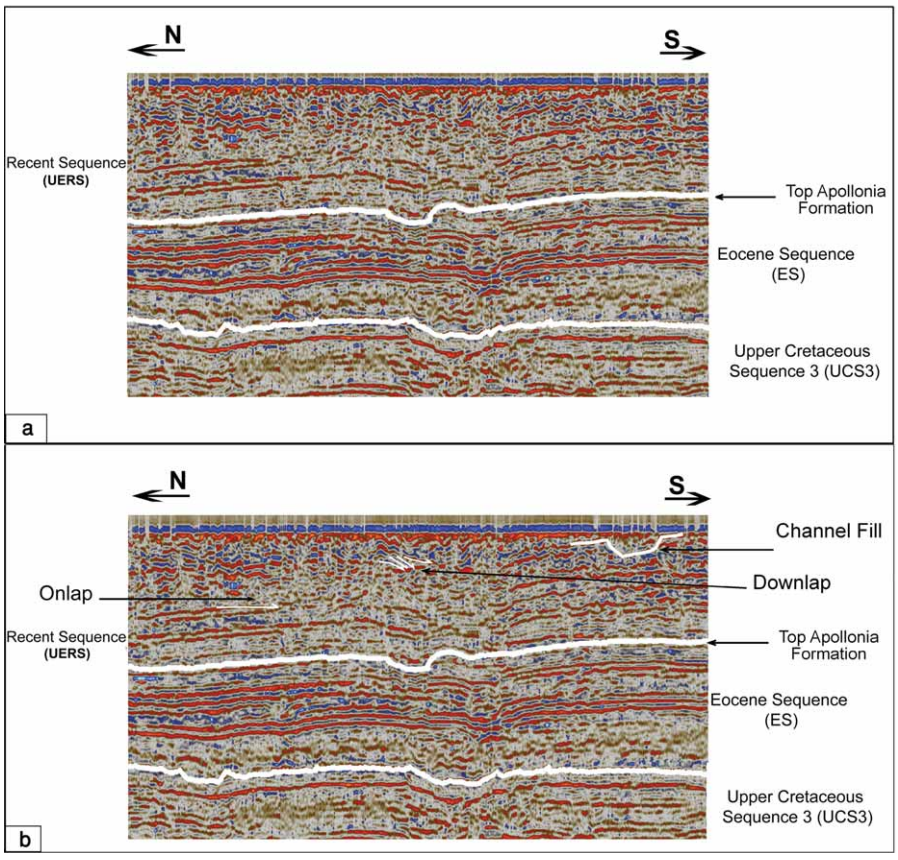

Figure 29: Showing the upper part of seismic line 5455 (west of the study area), (b): The interpreted seismic line 5455 displaying the main internal configurations which characterized the seismic facies of Upper Eocene to Recent Sequence (UERS).

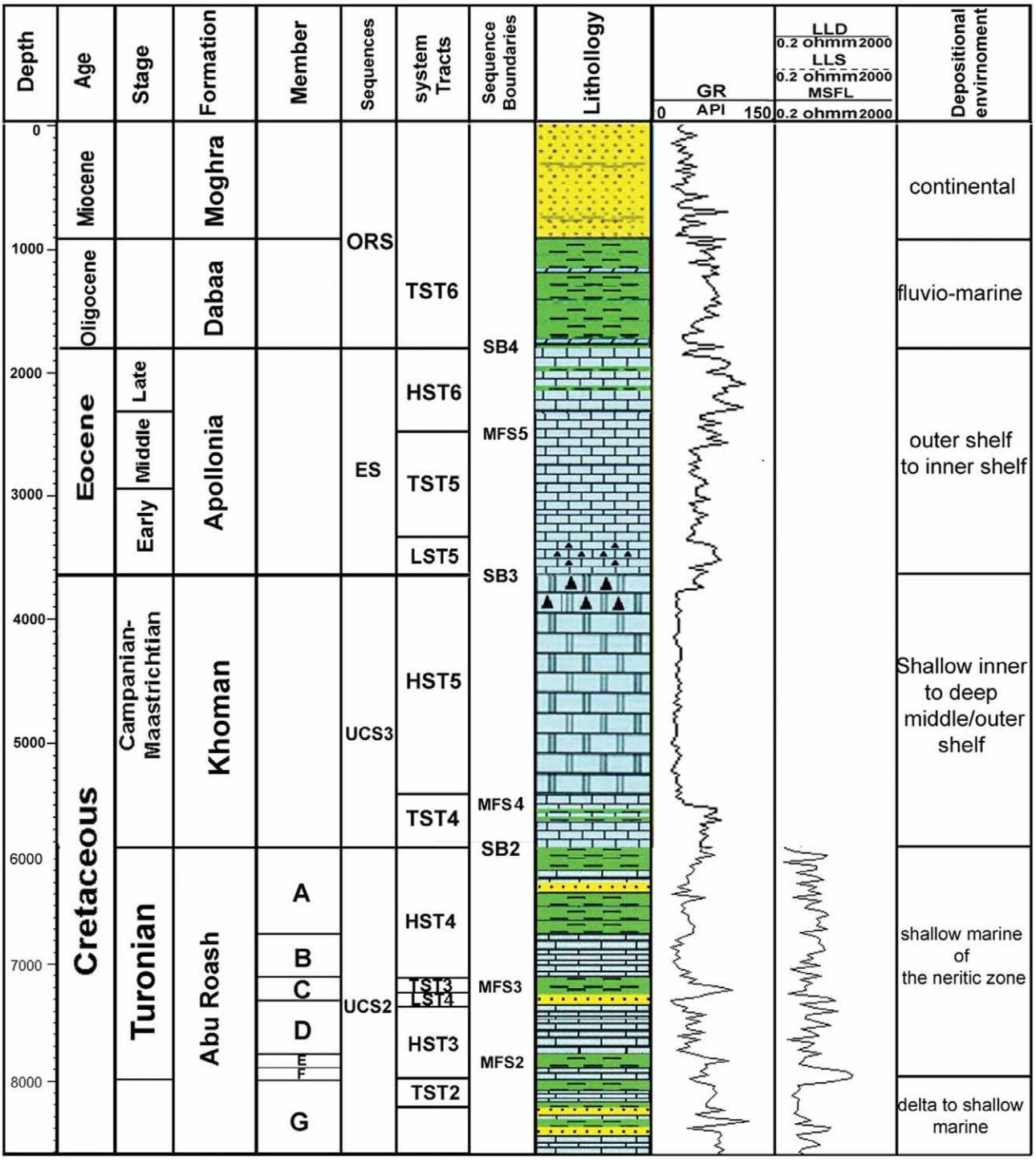

Figure 30: System tracts, logs and depositional environment of Turonian, Campanian–Maastrichtian, Eocene and Recent Sequences of Well Aqsa-1X.

in the central part of the studied area. The total thickness of this high system tract reach a maximum (30 m) in the Karma-SW 1x well and is minimal (18 m) in the in Karama-NW 5x well (Fig. 31).

6.1.3. Lowstand system tract (LST2)

This systems tract represents the second studied low system. It consists of a small part of the Abu Roash-G Member. The progradational LST2 sediments are characterized by low GR and relatively high resistivity**.**

Sediments of the LST2 are present all over the study area. The lithological composition of these deposits is mainly sandstone, mudstone and siltstone. The thickness of the LST2 sediments is quite small and uniform (about 10 m) (Fig. 31).

Seismic facies analysis and Gamma ray log confirm that the sandstone sediments indicate that, the prevalent environments of depositions during deposition of this system tract were estuaries or shorelines.

The sandstone units were most likely deposited as bay-head deltas, tidal channels and barrier beaches because they

display the characteristic features of tidal environments with a high dynamic regime of and wave influence.

6.1.4. Transgressive systems tract (TST1)

The retrogradational deposits of TST1 are marked by high GR and represents the onset of transgression and sea-level rise (NUMMEDAL & SWIFT, 1987). It overlies the transgressive surface (TS1), which tops the lowstand systems tract (LST1) (Fig. 31). The TST1 sediments are composed of shale and limestone deposits in most of the area and mainly shale with a few limestone interbeds in the West of the study area.

The maximum flooding surface (MFS1) separates the deposits of the retrograding interval of the TST1 below from the prograding deposits of the HST1 above (Fig. 31). This surface, together with the TST1 sediments, is associated with high peaks in the GR logs (SCHAFFER 1987; ARMENTROUT & CLEMENT, 1990).

The thickness of this system tract shows an increase in the middle part of the investigated area and decrease laterally in both sides (Fig. 31). Interpretation of seismic facies and Gamma ray log indicate that open marine conditions prevailing during the deposition of this system tract.

6.1.5. Highstand systems tract 2 (HST2)

This highstand system tract overlies the sediments of the transgressive systems tract TST1. Lithofacies of the HST2 sediments are clearly different to those of the HST1 sediments. HST2 sediments contain more shale in comparison with the HST1 (Fig. 31). The thickness of the HST2 sediments is quite variable. The maximum thickness (about 10 m) is detected at Aqsa-1X and K-SW-1X wells, while the minimum thickness (4 m) in K-NW-1X well (Fig. 31). From GR and lithology the prevailing environmental conditions during deposition of this system tract are deep marine conditions.

6.1.6. Lowstand system tract 3 (LST3)

The aggradational LST3 sediments have quite a similar well log response to those of the LST2 sediments (Fig. 31). The lithology of these deposits is mainly pro-delta silty-mudstone, lower, middle and upper shoreface sandstone, distributary-mouth bar sandstone, and distributary-channel sandstone, silty-muddy interdistributary or coastal plain deposits. The thickness of these deposits is quite variable with maximum thickness (about 12 m) drilled in K SW-1X and K SW-10X wells and minimum thickness (about 5 m) in K-NW-1X well. The log shape and the lithofacies characteristics of these sediments indicate that the LST3 sediments are deposited in similar conditions to those of the LST1.

6.1.7. Transgressive system tract 2 (TST2)

The retrogradational TST2 sediments have a quite different lithological composition and log response characteristics to those of the TST1. These sediments include the upper parts of the Abu Roach-G Member, composed of shale, limestones and sandstone respectively.

The upper boundary of the TST2 sediments is marked by an abrupt increase in the GR where the lower part shows low to moderate GR values. The increase of GR values in the upper part is due to an increase in the shale ratio within this system tract. The high shale content is attributed to the fact that, the Early Turonian started with the great transgres-

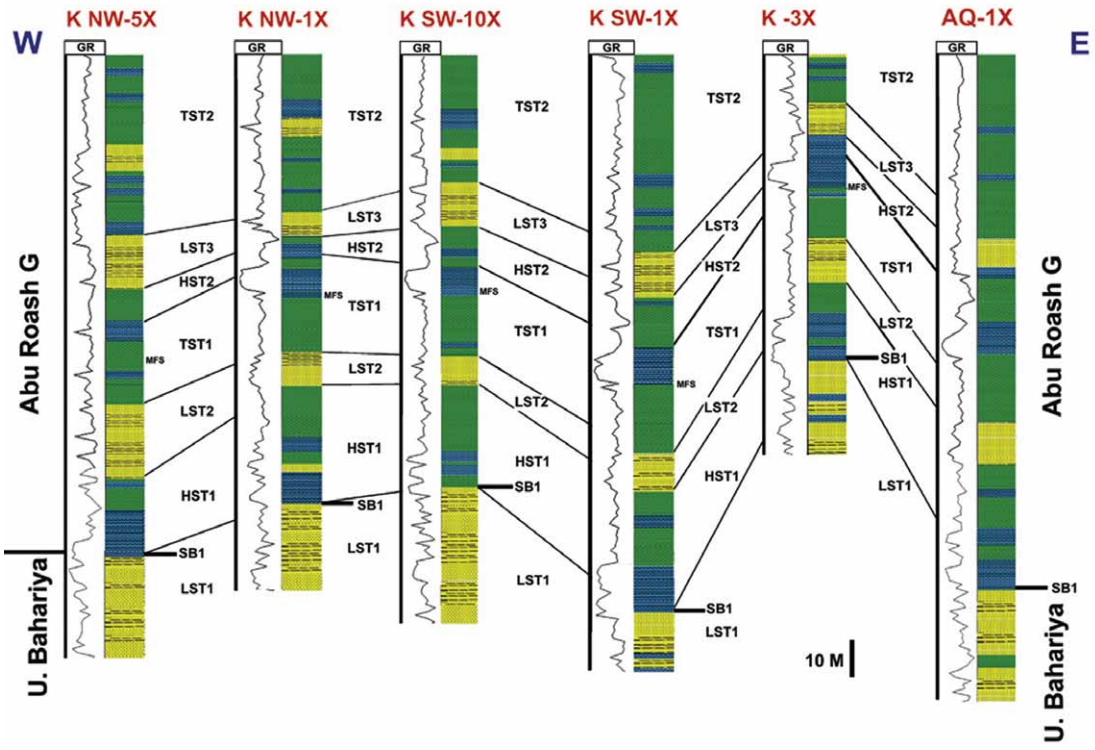

Figure 31: Schematic diagram for W-E correlation of the system tracks in the Abu Roash-G Member.

sion of the Late Cretaceous**,** which was recorded as the maximum flooding surface in the Western Desert (MFS2) (BARAKAT, 1987). The thickness of these deposits is quite variable with the maximum thickness of 60 m in well K-SW-1X.

6.2. Systems tracts of Turonian age

6.2.1. Highstand systems tract 3 (HST3)

This highstand system tract comprises the Abu Roash F, E and D Members. With the advent of the Turonian, the maximum flooding surface (MFS2) covered the northern part of the Western Desert (BARAKAT, 1987). This system tract tops the transgressive systems tract TST2 and represents the upper part of the Abu Roash-G Member.

Lithofacies of the HST3 sediments are similar to the HST1 sediments, composed mainly of shale and limestone (Figs. 26 and 29) where the Abu Roash members E, F and G are the most prolific and outstanding source rocks in the Western Desert (Lüning, 2004).

6.2.2. Lowstand systems tract 4 (LST4)

This lowstand systems tract is relatively thin representing part of the Abu Roash Fm. In the Turonian time (Figs. 26 and 29). It overlies the high stand system tract (HST3). The intervals of LST4 are characterized by a relatively decrease in gamma ray values.

This systems tract is part of the Abu Roash-C Member, composed of shale, sandstone and limestone indicating a shallow shelf marine (sublittoral) environment (ABDEL KHALEK, 1989).

6.2.3. Transgressive system tract 3 (TST3)

TST3 sediments have quite similar lithological well log characteristics to those of TST1, which is exclusively composed of shale and limestone sediments.

The upper boundary of the TST3 deposits is marked by moderate GR values. The second maximum flooding surface (MFS3) in Turonian time in the Western Desert is encountered directly above this system tract (Figs. 27 and 30).

This system tract is apart of the Abu Roash-D Member, which consists of limestone alternating with thin flint bands reflecting a shallow shelf marine environment (ABDEL KHALEK, 1989).

6.2.4. Highstand systems tract 4 (HST4)

This highstand systems tract occupies the top of the upper part of the Abu Roash Fm. and consists mainly of shale, limestone and sandstone intercalations and its deposits display moderate to high GR values, because the main lithological component is shale.

HST4 overlies the transgressive surface (MFS3), which tops the second transgressive systems tract of Turonian age. The predominant environmental conditions of deposition were those of shallow marine shelf (ABDEL KHALEK, 1989).

6.3. System tracts of Campanian–Maastrichtian age

6.3.1. Transgressive system tract 4 (TST4)

This transgressive systems tract represents the beginning of the sequence boundary (UCS3), which covers the high stand system tract sediments (HST4) high stand system tract sediments whereas the LST was truncated during the Coniacian and Santonian at the top of Khoman Formation due to subaerial exposure represented by an unconformity.

Lithofacies of the LST4 sediments are composed of sediments of limestones intercalated with shale which denotes the lower part of the Khoman Fm. (Figs. 27 and 30). The relatively deep sea conditions that prevailed by the offset of the Early Cenomanian persisted during the Late Cenomanian, Turonian and attained their peak in the Maastrichtian (BARAKAT, 1987) as reflected by the interpreted MFS4 surface. The TST4 is characterized by a strong increase in the gamma ray, which indicates an increase in sea level in the Western Desert (MFS4).

6.3.2. Highstand systems tract 5 (HST5)

This highstand systems tract represents the upper part of the Khoman Fm. and consists of open-marine white chalky limestone with chert bands.

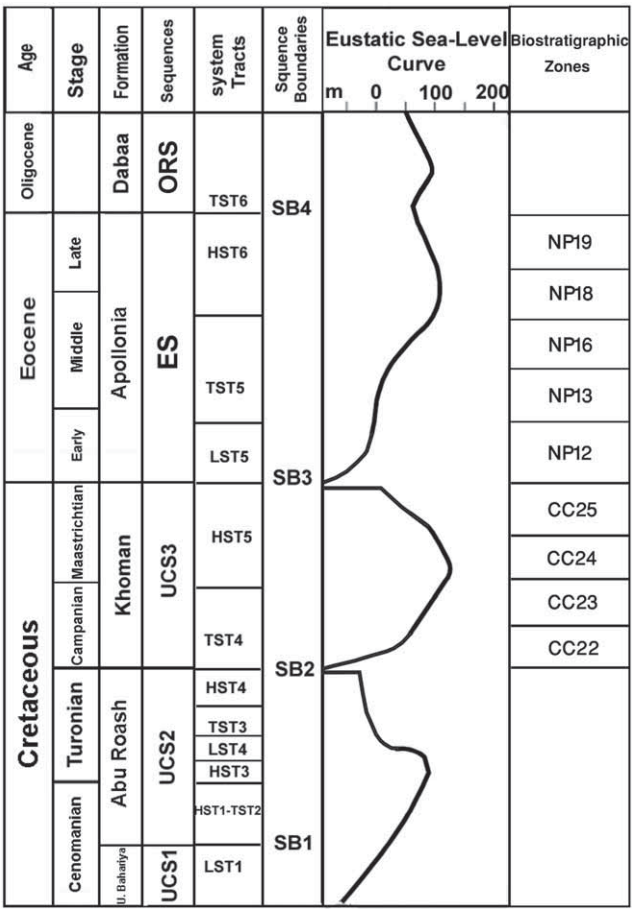

Figure 32: Formations, Sequences, Systems tracts and sea-level changes of the Upper Cretaceous-Eocene age of the subsurface East Bahariya succession.

It overlies the transgressive surface (MFS4), which tops the transgressive systems tract of Campanian-Maastrichtian age.

Data such as GR and fossil content indicate that the environmental conditions, which were prevailing during the deposition of the system tract, were indicative of a shallow inner shelf of marine environment.

6.4. Systems tracts of Eocene age

6.4.1. Lowstand systems tract 5 (LST5)

This lowstand system tract represents the lower part of the Apollonia Fm. (Figs. 27 and 30) wich overlies the sequence boundary (SB3), where It is tops the high stand systems tract (HST5).

The fossil content and available composite logs indicate that, this lowstand systems tract is composed of shallow marine limestone with numerous chert intervals. The cherty intervals of LST5 are characterized by a relative increase in gamma ray values. The high values are attributed to the concentration of organic matter within the chert beds.

The lithological, foraminiferal data and characteristics of the seismic reflectors of this sequence suggest that the depositional conditions in this systems tract range from outer shelf to inner shelf at the base of the Eocene period.

6.4.2. Transgressive systems tract 5 (TST5)

This transgressive systems tract includes the middle part of the Apollonia Formation. It overlies lowstand systems tract sediments (LST5) of the Eocene Sequence (ES). The MFS5 surface delineates the upper boundary of the retrograding sequence of the TST5 sediments. This surface is marked by the maximum GR response and the foraminiferal content (Figs. 27 & 30). The MFS5 is overlain by the prograding sequence of HST6 sediments.

This systems tract represents the maximum transgression recorded in the Western Desert area during the Middle-Late Eocene. Based on various types of available data the environmental conditions prevailing during the deposition of the system tract are outer shelf to inner shelf.

6.4.3. Highstand systems tract 6 (HST6)

This highstand systems tract consists of the upper part of the Eocene Sequence (ES) and represents the upper part of the Apollonia Fm. It is characterized by the abrupt increase of the Gamma ray values (Figs. 28 & 31). This increase in Gamma values is due to the high mud and silts fractions.

Highstand systems tract (HST6) overlies the maximum flooding surface MFS5, which tops the transgressive systems tract of Eocene age, where it includes limestone with shale interbeds. Limestone beds are rich in foraminifera which may indicate a deeper water habitat.

6.4.4. Transgressive systems tract 6 (TST6)

This transgressive systems tract includes the Dabaa Fm. It overlies the highstand systems tract (HST6) of the Eocene Sequence (ES). Transgressive system tract 6 (TST6) is characterized by an increase of gamma values with oscillation, but in the upper part gamma values suffer a moderate decrease compared to the lower part of this transgressive system tract (TST6).

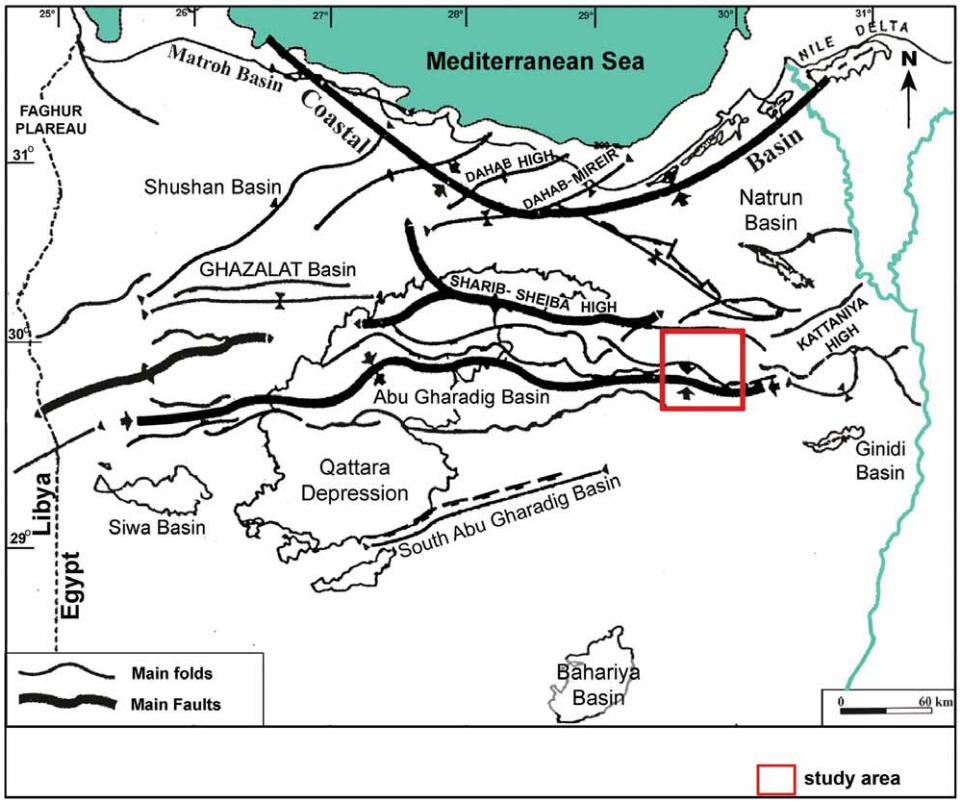

Figure 33: Illustrates the major structural trends in the Western Desert (after EGPC, 1992).

The available data suggest that the LST was removed due to marine erosion (TAWADROS, 2001). The environmental conditions, which were predominant during the deposition of this transgressive systems tract, were marine outer shelf to deep marine environments.

The aforementioned interpreted palaeo-environments of the study area exhibited echoes of the tectonic events affecting the southern margin of the Tethys Ocean. The study area, however, is located 80 Km offshore southern Tethys Ocean in the Abu Gharadig Basin, which is situated on the North African Plate. This basin developed in conjunction with a complex series of E-W and Northeast-Southwest oriented normal and wrench faults (Fig. 33) that formed during the Late Jurassic rifting and continued into, or were rejuvenated during the Early Cretaceous along the east Mediterranean margin resulting in the oceanization of the eastern Mediterranean basin. Rifting resulted from the initiation of the closure of the Tethys (GUIRAUD**,** 1998).

7. SUMMARY AND CONCLUSIONS

The calcareous nannofossils identified belong to CC22, CC23, CC25 of the Campanian – Maastrichtian age and zones NP12, NP13 of Early Eocene age and NP16 of Middle Eocene age and NP18 and NP19/20 of Late Eocene age. The ages of the different rock units were identified by means of planktonic foraminifera as well as calcareous nannofossils and some hiatuses were detected within the studied wells as follows:

1. The latest Cretaceous and the all of the Palaeocene are probably missing in the whole area, resulting in a major unconformity which may suggest tectonic instability due to pulses of epeirogenic movements affecting the area.
2. The boundary between the Apollonia Fm. and the overlying Dabaa Fm. is represented by an unconformity with corresponding hiatuses of different time spans. While the latest Eocene planktonic foraminifera such as *Cribrohantkenina*, *Turborotalia cerroazulensis cocoaensis*, *Turborotalia cerroazulensis cunialensis* are absent, it is possible to identify the Upper Eocene by means of the index calcareous nannofossils. The Apollonia Fm. (Campanian-Maastrichtian) rests unconformably on the Khoman Fm. (Eocene) in the study wells. The upper part of the Maastrichtian, as well as the entire Palaeocene, the basal part of the Eocene, and the upper part of the Middle Eocene are missing. The Eocene/Oligocene boundary could not be delineated due to the absence of nannofossil assemblages in the Dabaa Fm.
3. The Upper Cretaceous-Palaeogene succession for the studied area allows classification into five major 2nd order depositional sequences, separated by four major depositional sequence boundaries (SB1, SB2, SB3 and SB4). The Upper Cretaceous–Palaeogene succession in the East Bahariya is divided into 17 systems tracts. These systems tracts include: 7 System tracts of Cenomanian age; 4 System tracts of Turonian age, 2 System tracts of Campanian – Maastrichtian age and 4 System tracts of Eocene age.

ACKNOWLEDGEMENT

*The authors wish to express their deep gratitude to the Egyptian General Petroleum Corporation (EGPC) for releasing the seismic sections, composite logs, e-logs, cuttings on which the biostratigraphy is based and for providing the official permission to publish this work. The authors are deeply indebted to Professor Dr. Christian BETZLER, Geoscience Department, Hamburg University for his co-supervision through a Channel System of the Egyptian Mission Department. The Mission Department as well as Ain Shams University are greatly thanked. The authors thank Professor Dr.sc. Bruno SAFTIĆ, Faculty of Mining, Geology and Petroleum Engineering, University of Zagreb and the anonymous reviewer for reviewing the manuscript, their comments enhanced the quality of the manuscript. These thanks are extended to the Associate Editor, Professor Vlasta ĆOSOVIĆ, particularly Mme Alisa MARTEK and all the staff of GEOLOGIA CROATICA for their efforts.

REFERENCES

ABDEL AAL & MOUSTAFA, A.R. (1988): Structural framework in Abu El Gharadig Basin, Western Desert, Egypt.– In: EGPC – 9th Exploration Conference, Cairo, Egypt, p. 16.

ABDEL HAMID, M.L. (1985): Contribution to the Geology of Upper Cretaceous with special emphasis on Turonian-Senonian sedimentation patterns and hydrocarbon potentials in the Abu Gharadig Area, North Western Desert.– Unpubl. Ph.D. Thesis, Cairo University, 189 p.

ABDEL KHALEK, M.L., EL SHARKAWI, M.A., DARWISH, M., HAGRAS, M. & SEHIM, A. (1989): Structural history of Abu Roash district, Western Desert, Egypt.– J. African Earth Sci., 9/3–4, 435–443. doi: 10.1016/0899-5362(89)90027-4

ARMENTROUT, J.M. & CLEMENT, J.F. (1990): Biostratigraphic calibration of depositional cycles: a case study in High Island-Galveston-East Breaks, offshore Texas.– In: Sequence stratigraphy as an exploration Tool: concepts and practices in the Gulf Coast, SEPM, Gulf Coast Section – Eleventh Annual Research Conference – Program with Abstracts, 21–51.

AWAD, G.M. (1984): Habitat of oil in Abu Gharadig and Fayium Basins, Western Desert – Egypt.– B. Am. Assoc. Petrol. Geol., 68, 564–513.

BARAKAT, M.G., DARWISH, M. & ABDEL HAMID, M.L. (1984): Detection and Delineation of Reservoir Potential within Abu Roash Formation, East Abu Gharadig Area, North Western Desert, Egypt.– In: Abstracts of papers presented at the twenty-second Annual Meeting, Geol. Soc. of Egypt, 1.

BARAKAT, M.G., DARWISH, M. & ABDEL HAMID, M.L. (1987): Hydrocarbon source rock evaluation of Upper Cretaceous "Abu Roash Formation" east Abu Gharadig area; north Western Desert, Egypt.– In: M.E.R.C., Ain Shams University, Earth Science – Series -1, 120–150.

BAYOUMI, A.I. & LOTFY, H.I. (1989): Modes of structural evolution of Abu Gharadig Basin.– J. African Earth Sci., 9/2, 273–287. doi: 10.1016/0899-5362(89)90070-5

BAYOUMI, A.I., DARWISH, Y.A. & LOTFY, H.I. (1987): Acoustic characteristics of the Abu Gharadig Basin sediments.– J. African Earth Sci., 6/4, 399–405. doi: 10.1016/0899-5362(87) 90083-2

BAYOUMI, T. (1994): Synsedimentary tectonics & the distribution of Turonian sandstone reservoir, Abu Gharadig Basin, Western Desert, Egypt.– In: Proceedings of the EGPC 12th Petroleum Exploration & Production Conference, Cairo, 1, 368–387.

BAYOUMI, T. (1996): The influence of interaction of depositional environment and synsedimentary tectonics on the development of some Late Cretaceous source rocks, Abu Gharadig bash, Western Desert, Egypt.– In: Proceedings of the EGPC 13th Petroleum Exploration & Production Conference, Cairo, 2, 475–496.

BERGGREN, W.A. & PEARSON, P.N. (2006): Tropical to subtropical planktonic foraminiferal zonation of the Eocene and the Oligocene.– In: PEARSON, P.N. et al. (eds.): Atlas of Eocene Planktonic Foraminiferas. Cushman Found. Spec. Publ., 41, 29–40.

BLOW, W.H. (1979): The Cenozoic Globigerinida: A Study of the Morphology, Taxonomy, Evolutionary Relationships and the Stratigraphical Distribution of some Globigerinida (mainly Globigerinacea).– E. J. Brill, Leiden, 1413 p.

BOLLI, H.M. (1957B): Planktonic foraminifera from the Oligocene – Miocene Cipero and Lengua Formations of Trinidad, B.W.I.– In: LOEBLICH, A.R. et al. (eds.): Studies in Foraminifera. U.S. Natural Museum Bulletin, 215, 97–123.

BRONNIMANN, P. & STRADNER, H. (1960): Die Foraminiferen – und Discoasteridenzonen von Kuba und ihre interkontinentale Correlation.– Erdoel-Z., 76, 364–369.

BUKRY, D. & BRAMLETTE, M.N. (1970): Coccolith age determinations, Leg 3, Deep Sea Drilling Project.– In: Deep Sea Drilling Project, 3, 589–611. doi: 10.2973/dsdp.proc.3.118.1970

BUKRY, D. (1973A): Coccolith stratigraphy, Leg 10, Deep Sea Drilling Project.– In: Deep Sea Drilling Project, 10, 385–604. doi:10.2973/dsdp.proc.10.117.1973

BUKRY, D. (1973B): Low latitude coccolith biostratigraphic zonation.– In: Deep Sea Drilling Project, 15, 685–703. doi:10.2973/dsdp.proc.15.116.1973

CARON, M. (1985): Cretaceous planktic foraminifera.– In: BOLLI, H.M., SAUNDERS, J.B. & PERCH-NIELSEN, K. (eds.): Plankton Stratigraphy, Cambridge University Press, 17–86.

CARON, M., AGNOLO, S.D., ACCARIE, H., BARRERA, E., KAUFFMAN, E.G., AMÉDRO, F. & ROBASZYNSKI, F. (2006): High-resolution stratigraphy of the Cenomanian – Turonian boundary interval at Pueblo (USA) and Wadi Bahloul (Tunisia): Stable isotope and bio-events correlation.– Geobios, 39, 171–200. doi: 10.1016/j.geobios.2004.11.004

CATUNEANU, O., KHALIFA, M.A. & WANAS, H.A. (2006): Sequence stratigraphy of the Lower Cenomanian Bahariya Formation, Bahariya Oasis, Western Desert, Egypt.– Sediment. Geol., 190, 121–137. doi:10.1016/j.sedgeo.2006.05.010

DARWISH, M., ABU KHADRAH, A.M., ABDEL HAMID, M.L. & HAMED, T.A. (1994): Sedimentology, environment conditions and hydrocarbon habitat of the Bahariya Formation, central Abu Gharadig Basin, Western Desert, Egypt.– In: Proc. of EGPC 12th Petrol. Exploration & Production Conference, Cairo, Egypt, 1, 429–449.

EGPC (1992): Western Desert Oil and Gas Fields (A Comprehensive Overview): EGPC – 11th Exploration Conference.– EGCP, Cairo, Egypt, 431 p.

EL BASSYOUNY, A.A. (1970): Geology of the area between Gara El Hamra of Ball-Qur Lyons and Ghard El Moharrik, and its correlation with El Harra area, Bahariya Oasis, Egypt.– Unpubl. MSc Thesis, Cairo University, 180 p.

EMERY, D. & MYERS, K.J. (1996): Sequence Stratigraphy.– Blackwell, Oxford, 297 p. doi:10.1002/9781444313710

GHANEM, M.F. (1985): Subsurface Geology of the Cretaceous sediments in the North Western Desert of Egypt and its hydrocarbon potentialities.– Unpubl. PhD. Thesis, Faculty of Science, Cairo University, 131 p.

GUIRAUD, R. (1998): Mesozoic rifting and basin inversion along the northern African Tethyan margin: an overview.– In: MACGREGOR, D.S., MOODY, R.T.J. & CLARK-LOWES, D.D. (eds.): Petroleum Geology of North Africa, London, Geological Society Special Publication, 132, 217–229. doi:10.1144/GSL.SP.1998.132.01.13)

HARPE DE LA (1883): Monographie der in Ägypten und der libyschen wüste von kommenden Nummuliten.– Paleontographica, 30, 155–216.

HAY, W.W., MOHLER, H.P., ROTH, P.H., SCHMIDT, R.R., & BOUDREAUX, J.E. (1967): Calcareous nannoplankton zonation of the Cenozoic of the Gulf Coast and Caribbean-Antillean area and transoceanic correlation: Gulf Coast Assoc.– Geological Society Transactions, 17, 428–480.

HAY, W.W., MOHLER, H.P. & WADE, M.E. (1966): Calcareous nannofossils from Nal' chik (northwest Caucasus).– Eclogae Geol. Helvet., 59, 379–399.

ISMAIL, M.M., EL NOZAHY, F.A. & SADEEK, K.N. (1989): A contribution to the geology of the Bahariya Oasis, Western Desert, Egypt.– Geological Journal, 18/4, 379–391. doi:10.1007/BF00772692

ISSAWI, B., FRANCIS, M.H., YOUSSEF, E.A.A., & OSMAN, R.A. (2009): The Phanerozoic Geology of Egypt: A Geodynamic Approach: Special publication, 81.– Ministry of Petroleum, Cairo, 589 p.

ISSAWI, B., HINNAWI, M., FRANCIS, M. & MAZHAR, A. (1999): The Phanerozoic geology of Egypt: a geodynamic approach.– Geological Survey of Egypt, Cairo, 462 p.

SMITH JOSHUA, B., LAMANNA MATHEW, C., HELMUT M. & LACOVARA KENNETH, J. (2006): New information regarding the holotype of *SPINOSAURUS AEGYPTIACUS* STROMER, 1915.– J. Paleontol., 80/2, 400–406.

LÜNING, S., ADAMSON, K. & CRAIG, J. (2003): Frasnian organic-rich shales in North Africa: regional distribution and depositional mode.– In: ARTHUR, T.J., MACGREGOR, D.S. & CAMERON, N. (eds.): Petroleum Systems and Emerging Technologies in African Exploration and Production, Special Publication of the Geological Society, 207, 165–184. doi: 10.1144/ GSL.SP.2003.207.01.09

PASLEY, M.A., ARTIGAS, G., NASSEF, O. & COMISKY, J. (2009): Depositional Facies Control on Reservoir Characteristics in the Middle and Lower Abu Roash „G" Sandstones, Western Desert, Egypt.– Search and Discovery Article #50181, Posted May 8, 2009. Adapted from oral presentation at AAPG International Conference and Exhibition, Cape Town, South Africa, October 26–29, 2008.

MARTINI, E. (1971): Standard Tertiary and Quaternary calcareous nannoplankton zonation.– In: FARINACCI, A. (ed.): Proc. II Planktonic Conference, Roma, 2, 739–785.

MARTINI, E. (1976): Cretaceous to recent calcareous nannoplankton from the central Pacific Ocean.– In: Deep Sea Drilling Project, 33, 383–423.

NORTON, P. (1967): Rock-stratigraphic nomenclatures of the Western Desert, Egypt.– Egyptian Petroleum Corporation, Cairo, 557 p.

NUMMEDAL, D. & SWIFT, D.J.P. (1987): Transgressive stratigraphy at sequence bounding unconformities.– In: NUMMEDAL et al. (eds.): Sea Level Fluctuations and Coastal Evolution, SEPM Special Publication, 41, 241–260. doi:10.2110/pec.87.41.0241

OKADA, H. & BUKRY, D. (1980): Supplementary modification and introduction of code numbers to the low latitude coccolith biostratigraphic zonation (BUKRY, 1973, 1975).– Mar. Micropaleontol., 5, 321–325. doi:10.1016/0377-8398(80)90016-X

OSMAN, R.A. (2003): Contribution to the stratigraphy of El Arag depression, North Western Desert, Egypt.– Sedimentology of Egypt, 11, 157–167.

PERCH-NIELSEN, K. (1972): Remarks on Late Cretaceous to Pleistocene coccoliths from the North Atlantic.– In: Deep Sea Drilling Project, 12, 1003–1069. doi:10.2973/dsdp.proc.12.115.1972

PERCH-NIELSEN, K. (1985A)**:** Mesozoic calcareous nannofossils.– In: BOLLI, H.M., SAUNDERS, J.B. & PERCH-NIELSEN, K. (eds.):

Plankton Stratigraphy, Cambridge Univ. Press, Cambridge, 329–4. doi:10.2973/dsdp.proc.12.115.1972

SAID, R. (1962): The geology of Egypt.– Elsevier, Amsterdam, 377 p.

SAID, R. (1960): Planktonic foraminifera from the Thebes Formation, Luxor, Egypt.– Micropaleontology, 6, 277–286. doi:10.2307/1484234

SCHAFFER, B.L. (1987): The potential of calcareous nannofossils for recognizing Plio-Pleistocene climatic cycles and sequence boundaries on the shelf.– In: Eighth Annual Research Conference, Gulf Coast Section SEPM Foundation, 142–145.

SCHLUMBERGER (1984A): Well evaluation conference, Egypt.– Schlumberger Limited, New York, 250 p.

SISSINGH, W. (1977): Biostratigraphy of Cretaceous calcareous nannoplankton.– Geologie en mijnbouw, 56/1, 37–65.

STROMER, E. (1914): Die Togographi und Geologie der Strecke Gharaq – Baharije nebest Ausfuhrungen ueber die geologische Geschichte Aegyptens.– Abh. Bayer, Akad. Wissensch., Math.: Naturw. Kl., 11, 1–78.

TAWADROS, E.E. (2001): Geology of Egypt and Libya.– Balkema, Rotterdam, 468 p.

TOUMARKINE, M. & LUTRBACHER, H. (1985): Paleocene and Eocene planktic foraminifera.– In: BOLLI, H.M., SAUNDERS, J.B., & PERCH-NIELSEN, K. (eds.): Plankton Stratigraphy, Cambridge Univ. Press, Cambridge, 87–154.

VAN WAGONER, J.C., POSAMENTIER, H.W., MITCHUM, R.M., VAIL, P.R., SARG, J.F., LOUTIT, T.S. & HARDENBOL, J. (1988): An overview of the fundamentals of sequence stratigraphy and key definitions.– In: WILGUS, C.K. et al. (eds.): Sea – Level Changes: An Integrated Approach, Special Publication of the Society of Eocene Paleontology, Mineral, 42, 39–45.

YOUNES, M.A. (2003): Alamein Basin Hydrocarbon Potentials, Northern Western Desert, Egypt (Extended Abstract).– In: AAPG Annual Convention, May 11–14, 2003, Salt Lake City, Utah, p. 6.

Manuscript received March 3, 2011
Revised manuscript accepted March 04, 2012
Available online June 29, 2012